Monthly Notices
of the
ROYAL ASTRONOMICAL SOCIETY

MNRAS **435,** 1325–1349 (2013)
Advance Access publication 2013 August 20

doi:10.1093/mnras/stt1375

Re-examining the membership and origin of the ϵ Cha association

Simon J. Murphy,[1,2]★ Warrick A. Lawson[3] and Michael S. Bessell[2]

[1]*Gliese Fellow, Astronomisches Rechen-Institut, Zentrum für Astronomie der Universität Heidelberg, D-69120 Heidelberg, Germany*
[2]*Research School of Astronomy and Astrophysics, Australian National University, Canberra, ACT 2611, Australia*
[3]*School of Physical, Environmental and Mathematical Sciences, University of New South Wales, Canberra, ACT 2600, Australia*

Accepted 2013 July 22. Received 2013 July 5; in original form 2013 May 15

ABSTRACT

We present a comprehensive investigation of the ϵ Chamaeleontis association (ϵ Cha), one of several young moving groups spread across the southern sky. We re-assess the putative membership of ϵ Cha using the best available proper motion and spectroscopic measurements, including new ANU 2.3-m/Wide Field Spectrograph observations. After applying a kinematic analysis, our final membership comprises 35–41 stars from B9 to mid-M spectral types, with a mean distance of 110 ± 7 pc and a mean space motion of $(U, V, W) = (-10.9 \pm 0.8, -20.4 \pm 1.3, -9.9 \pm 1.4)$ km s^{-1}. Theoretical evolutionary models suggest ϵ Cha is 3–5 Myr old, distinguishing it as the youngest moving group in the solar neighbourhood. 15 members show 3–22 μm spectral energy distributions attributable to circumstellar discs, including 11 stars which appear to be actively accreting. ϵ Cha's disc and accretion fractions (29^{+8}_{-6} and 32^{+9}_{-7} per cent, respectively) are both consistent with a typical 3–5 Myr old population. Multi-epoch spectroscopy reveals three M-type members with broad and highly variable Hα emission as well as several new spectroscopic binaries. We reject 11 stars proposed as members in the literature and suggest they may belong to the background Cha I and II clouds or other nearby young groups. Our analysis underscores the importance of a holistic and conservative approach to assigning young stars to kinematic groups, many of which have only subtly different properties and ill-defined memberships. We conclude with a brief discussion of ϵ Cha's connection to the young open cluster η Cha and the Scorpius–Centaurus OB association (Sco–Cen). Contrary to earlier studies which assumed η and ϵ Cha are coeval and were born in the same location, we find the groups were separated by ∼30 pc when η Cha formed 4–8 Myr ago in the outskirts of Sco–Cen, 1–3 Myr before the majority of ϵ Cha members.

Key words: stars: formation – stars: kinematics and dynamics – stars: low-mass – stars: pre-main sequence – open clusters and associations: individual: ϵ Chamaeleontis, η Chamaeleontis.

1 INTRODUCTION

Young stars in the solar neighbourhood are ideal laboratories for studying circumstellar discs and nascent planetary systems at high resolution and sensitivity. Well-characterized samples of stars with ages $\lesssim$10 Myr are particularly important, as it is during these epochs that discs rapidly evolve from massive gas-rich systems capable of supporting accretion and the formation of giant planets, to more-quiescent dusty debris discs which are the precursors of terrestrial planets. (e.g. Haisch, Lada & Lada 2001; Williams & Cieza 2011).

Members of nearby ($\lesssim$100 pc) kinematic associations, like those around the young stars TW Hydrae (age 8–10 Myr) and β Pictoris (∼12 Myr), have proven fruitful targets for such work (Zuckerman & Song 2004; Torres et al. 2008). However, the majority of stars in these groups show signs that their primordial discs are already evolved (Schneider, Melis & Song 2012a; Simon et al. 2012). With an age of 3–5 Myr (see Section 6.2), the ϵ Chamaeleontis association (Mamajek, Lawson & Feigelson 2000; Feigelson, Lawson & Garmire 2003) is therefore ideally suited to studies of the rapid disc evolution taking place at these intermediate ages (Sicilia-Aguilar et al. 2009; Fang et al. 2013).

However, because of ϵ Cha's greater distance (100–120 pc), compared to other nearby young groups, southern declination and position in the foreground of the Chamaeleon molecular cloud complex (170–210 pc, age 2–4 Myr; Luhman 2008), it has suffered from somewhat of an identity crisis in the literature. Over 50 members of a putative moving group in the region have been proposed in the past 15 years and there are several overlapping definitions of this group in the literature. Many candidates lack radial velocities necessary for confirming membership in a moving group and several stars have no spectroscopy at all. If ϵ Cha is a true coeval association

★ E-mail: murphy@ari.uni-heidelberg.de

then all of its members must have consistent age indicators (e.g. X-ray and Hα emission, lithium depletion, elevated colour–magnitude diagram (CMD) position, low surface gravity; Zuckerman & Song 2004) and space motions (via proper motions and radial velocities) consistent with being a comoving ensemble.

In this contribution, we attempt to clarify the situation by critically re-examining the membership of ϵ Cha. The structure of this paper is as follows. In Section 2, we outline the various members proposed in the literature. The properties and kinematics of these stars are described in Sections 3 and 4, including new multi-epoch spectroscopy. Applying a kinematic and colour–magnitude analysis (Section 5), we present the new membership of ϵ Cha in Section 6, with a discussion of its age, circumstellar discs and binaries. We conclude by discussing ϵ Cha's relationship to the open cluster η Chamaeleontis and their origin in the Scorpius–Centaurus OB association (Sco–Cen) (Section 7).

2 ϵ CHA IN THE LITERATURE

2.1 Early work

The ϵ Cha association has existed in the literature in various guises for 15 years. Frink et al. (1998) discovered several young *ROSAT* sources between the Cha I and II dark clouds (Fig. 2) with proper motions that placed them much closer to the Sun ($d \approx 90$ pc, their 'subgroup 2'). Terranegra et al. (1999) subsequently identified 13 stars between the clouds with similar proper motions, which they claimed formed a distinct kinematic association. They derived a distance of 90–110 pc and an isochronal age of 5–30 Myr.

While investigating the young open cluster η Cha (Mamajek, Lawson & Feigelson 1999), Mamajek et al. (2000) also looked at stars in the vicinity of ϵ Cha and HD 104237. They identified eight stars with congruent proper motions and photometry, and used several with radial velocities and parallaxes to derive a space motion for the group.

Feigelson et al. (2003) then obtained *Chandra X-ray Observatory* snapshots of two fields around HD 104237, finding four low-mass companions to the Herbig Ae star at separations of 160–1700 au and three more spectroscopically young mid-M stars at larger separations. Luhman (2004b) soon added another three lithium-rich low-mass stars in the vicinity. These 12 stars constitute the 'classical' membership of ϵ Cha.

In their review of young stars near the Sun, Zuckerman & Song (2004) proposed a $\sim$10 Myr old group surrounding (but not including) ϵ Cha and HD 104237 which they called 'Cha-Near'. It included six new candidates and 11 stars from the memberships of Terranegra et al. (1999) and Mamajek et al. (2000). While Zuckerman & Song considered Cha-Near and the aggregate around ϵ Cha/HD 104237 to be separate groups, it is now apparent they are all members of the same spatially extended association.

Finally, while investigating the disc properties of Cha I members with the *Spitzer Space Telescope*, Luhman et al. (2008) identified four stars with proper motions consistent with membership in the ϵ Cha association defined by Feigelson et al. (2003), and several new *ROSAT* sources not previously attributed to ϵ Cha.

2.2 Torres et al. (2008) compilation

Torres et al. (2008) reviewed ϵ Cha as part of their ongoing programme to identify new members of young, loose associations (see also Torres et al. 2006). Using radial velocities from the literature and their own observations, they proposed 24 high-probability members with congruent kinematics, photometry and lithium absorption. Their solution included 14 stars from the previously described studies, six new members and four members of the open cluster η Cha (RECX 1, 8, 12 and η Cha itself). Torres et al. considered η Cha to be a part of ϵ Cha and while the two groups have similar ages, distances and kinematics, in this work we consider only the 20 stars they classified as ϵ Cha 'field members'. We will discuss the relationship between η and ϵ Cha in greater detail in Section 7.1.

Of the candidates not proposed as members by Torres et al. (2008), they rejected only three;[1] RX J1150.4−7704 (ϵ Cha 19; Terranegra et al. 1999) had kinematics far from their convergent solution, HIP 55746 (Zuckerman & Song 2004) was reclassified as a member of the AB Doradus association and RX J1158.5−7754A (ϵ Cha 21; Terranegra et al. 1999) was a poor kinematic match at its 90 pc *Hipparcos* distance. The remaining stars lacked radial velocities necessary for the convergence method. Measuring velocities for these stars is one of the key contributions of this work.

2.3 New candidates

Several new members of ϵ Cha have been proposed since the compilation of Torres et al. (2008). Kiss et al. (2011) suggested 2MASS J12210499−7116493 as a new member at an estimated kinematic distance of 98 pc. The star has strong Li I λ6708 absorption and a velocity only 1.5 km s^{-1} from the Torres et al. space motion.[2] Kastner et al. (2012) then identified 2MASS J11550485−7919108 as a wide (0.2 pc), comoving companion to T Cha (Frink et al. 1998). Both stars are young and host circumstellar material. Most recently, Lopez Martí et al. (2013) reanalysed the proper motions of young stars in Chamaeleon and proposed the new ϵ Cha member RX J1216.8−7753 as well as reclassifying the Cha II star CM Cha as a potential member of the association.

After tracing back in time the positions of nearby ($d < 30$ pc) *Hipparcos* stars with present-day space motions similar to local moving groups, Nakajima & Morino (2012) proposed an additional seven members of the 'Cha-Near' association of Zuckerman & Song (2004). By considering only coarse youth indicators (variability, X-ray emission) their new 'members' include the older pre-main-sequence stars GJ 82 (estimated age 35–300 Myr; Shkolnik, Liu & Reid 2009), DK Leo (>400 Myr; Shkolnik et al. 2009), GJ 755 (200 ± 100 Myr; Barrado y Navascues 1998), HR 3499 (>100 Myr; Wichmann, Schmitt & Hubrig 2003), the β Pic member AF Lep (Torres et al. 2008) and the binary EQ Peg, whose M3.5 primary has only a marginal lithium detection (Zboril, Byrne & Rolleston 1997), implying an age greater than 10 Myr. Given their current locations, older ages and that none of the stars were closer than $\sim$20 pc from the centre of Cha-Near 10 Myr ago (the age assumed for the group), they are almost certainly not true members of Cha-Near or ϵ Cha and we discuss them no further.

Excluding the Nakajima & Morino candidates there are 52 putative members of the 'ϵ Cha association' in the literature. They are listed in Table 1 with spectral types and membership references. Their astrometry has been resolved against Two Micron All Sky

[1] Torres et al. did not test the membership of VW Cha, the only Frink et al. (1998) candidate not also included by Terranegra et al. (1999).

[2] Kiss et al. swapped the radial velocity of 2MASS J1221−71 with the β Pic member 2MASS J01071194−1935359 in their table 1. The listed space motions for both stars are consistent with their correct velocities.

Table 1. Proposed members of the ϵ Cha association from the literature.

ID[a]	Name	Right ascension (J2000)	Declination (J2000)	Spectral type[d]	V [d] (mag)	Membership[b] references	Torres et al. member?
	HD 82879	09 28 21.1	−78 15 35	F6	8.99	8	Y
	CP−68 1388	10 57 49.3	−69 14 00	K1	10.39	8	Y
	VW Cha	11 08 01.5	−77 42 29	K8	12.64	1	
	TYC 9414-191-1	11 16 29.0	−78 25 21	K5	10.95	3	
13	2MASS J11183572−7935548	11 18 35.7	−79 35 55	M4.5	14.91	7	
14	RX J1123.2−7924	11 22 55.6	−79 24 44	M1.5	13.71	7	
	HIP 55746	11 25 18.1	−84 57 16	F5	7.6	6	
15	2MASS J11334926−7618399	11 33 49.3	−76 18 40	M4.5	–	7	
	RX J1137.4−7648	11 37 31.3	−76 47 59	M2.2	–	6	
16	2MASS J11404967−7459394	11 40 49.7	−74 59 39	M5.5	17.28	7	
	TYC 9238-612-1	11 41 27.7	−73 47 03	G5	10.7	6	
17	2MASS J11432669−7804454	11 43 26.7	−78 04 45	M4.7	17.33	7	
	RX J1147.7−7842	11 47 48.1	−78 41 52	M3.5	–	6	
18	RX J1149.8−7850	11 49 31.9	−78 51 01	M0	12.9	7	Y
19	RX J1150.4−7704	11 50 28.3	−77 04 38	K4	12.0	1,2,6,7	
	RX J1150.9−7411[c]	11 50 45.2[c]	−74 11 13[c]	M3.7	14.4	2	
	2MASS J11550485−7919108	11 55 04.9	−79 19 11	M3	–	10	
	T Cha	11 57 13.5	−79 21 32	K0	12.0	1,2,6	Y
20	RX J1158.5−7754B	11 58 26.9	−77 54 45	M3	14.29	7	Y
21	RX J1158.5−7754A	11 58 28.1	−77 54 30	K4	10.9	1,2,3,6,7	
	HD 104036	11 58 35.4	−77 49 31	A7	6.73	3,6	Y
1	CXOU J115908.2−781232	11 59 08.0	−78 12 32	M4.75	–	4	
2	ϵ Cha AB	11 59 37.6	−78 13 19	B9	5.34	3,4	Y
	RX J1159.7−7601	11 59 42.3	−76 01 26	K4	11.31	1,2,3,6	Y
3	HD 104237C	12 00 03.6	−78 11 31	M/L	∼25	4	
4	HD 104237B	12 00 04.0	−78 11 37	K/M	15.1	4	
5	HD 104237A	12 00 05.1	−78 11 35	A7.75	6.73	2,3,4	Y
6	HD 104237D	12 00 08.3	−78 11 40	M3.5	14.28	4	Y
7	HD 104237E	12 00 09.3	−78 11 42	K5.5	12.08	4	Y
10	2MASS J12005517−7820296	12 00 55.2	−78 20 30	M5.75	–	5	
	HD 104467	12 01 39.1	−78 59 17	G3	8.56	1,2,6	Y
11	2MASS J12014343−7835472	12 01 43.4	−78 35 47	M2.25	–	5	
8	USNO-B 120144.7−781926	12 01 44.4	−78 19 27	M5	–	4	
9	CXOU J120152.8−781840	12 01 52.5	−78 18 41	M4.75	–	4	
	RX J1202.1−7853	12 02 03.8	−78 53 01	M0	12.48	8	Y
	RX J1202.8−7718	12 02 54.6	−77 18 38	M3.5	14.4	2,6	
	RX J1204.6−7731	12 04 36.2	−77 31 35	M3	13.81	2,6	Y
	TYC 9420-676-1	12 04 57.4	−79 32 04	F0	10.28	3	
	HD 105234	12 07 05.5	−78 44 28	A9	7.4	3	
12	2MASS J12074597−7816064	12 07 46.0	−78 16 06	M3.75	–	5	
	RX J1207.7−7953	12 07 48.3	−79 52 42	M3.5	14.5	6	
	HIP 59243	12 09 07.8	−78 46 53	A6	6.9	6	
	HD 105923	12 11 38.1	−71 10 36	G8	9.16	8	Y
	RX J1216.8−7753	12 16 45.9	−77 53 33	M4	13.88	11	
	RX J1219.7−7403	12 19 43.5	−74 03 57	M0	13.08	2,6	Y
	RX J1220.4−7407	12 20 21.9	−74 07 39	M0	12.85	2,6	Y
	2MASS J12210499−7116493	12 21 05.0	−71 16 49	K7	12.16	9	
	RX J1239.4−7502	12 39 21.2	−75 02 39	K3	10.30	2,6	Y
	RX J1243.1−7458[c]	12 42 53.0[c]	−74 58 49[c]	M3.2	15.1	2	
	CD−69 1055	12 58 25.6	−70 28 49	K0	9.95	8	Y
	CM Cha	13 02 13.6	−76 37 58	K7	13.40	11	
	MP Mus	13 22 07.6	−69 38 12	K1	10.35	8	Y

[a] ϵ Cha identification number (Feigelson et al. 2003; Luhman 2004b, SIMBAD: [FLG2003] EPS CHA #).
[b] Membership references: (1) Frink et al. (1998), (2) Terranegra et al. (1999), (3) Mamajek et al. (2000), (4) Feigelson et al. (2003), (5) Luhman (2004b), (6) Zuckerman & Song (2004), (7) Luhman et al. (2008), (8) Torres et al. (2008), (9) Kiss et al. (2011), (10) Kastner et al. (2012), (11) Lopez Martí et al. (2013)
[c] Updated coordinates to those presented by Alcala et al. (1995).
[d] Spectral types from the literature (see Table B1) and our WiFeS observations. Indicative V magnitudes from SIMBAD.

Survey (2MASS) images and our own spectroscopic observations. For candidates proposed by Feigelson et al. (2003), Luhman (2004b) and Luhman et al. (2008), we provide the ϵ Cha identification number (1–21) used in those studies. Figs 1 and 2 show the location of ϵ Cha candidates on the sky. While the region around ϵ Cha and HD 104237 (Fig. 1) is well studied, the majority of the dispersed population are isolated *ROSAT* sources or incidental observations of stars around the Cha I cloud. Given the shallow depth of the

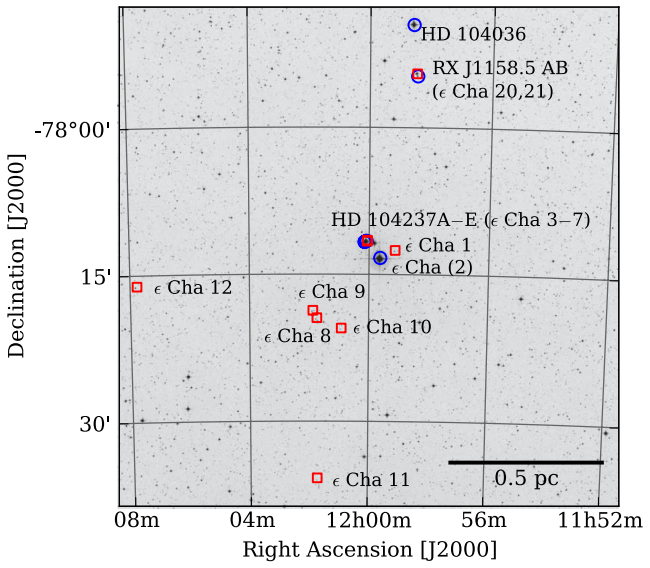

Figure 1. POSS2-IR 1 deg^2 image centred on ϵ Cha AB ($11^h59^m37\overset{s}{.}6, -78°13'19''$, J2000) with proposed association members from the literature (red squares) and kinematic members from Torres et al. (2008) (blue circles). The scale uses the 111 pc distance to ϵ Cha.

flux-limited *ROSAT* All Sky Survey, future studies may reveal additional X-ray-faint members across the region.

3 OBSERVATIONS OF CANDIDATE MEMBERS

3.1 WiFeS multi-epoch spectroscopy

Many of the proposed ϵ Cha members lack radial velocities necessary for confirming membership in a moving group. To remedy this and assess the youth of the candidates, we observed 19 K and M-type stars from Table 1 with the Wide Field Spectrograph (WiFeS; Dopita et al. 2007) on the ANU 2.3-m telescope at Siding Spring. To constrain any velocity variations and investigate circumstellar accretion (Murphy et al. 2011), we observed each star three to seven times over 60–480 d between 2010 February and 2011 June. We used the *R*7000 grating, which gave $\lambda/\Delta\lambda \approx 7000$ and coverage from 5300 to 7100 Å. Exposure times were 900–5400 s per epoch. To estimate spectral types, surface gravities and reddenings, we also obtained single-epoch *R*3000 spectra (5300–9600 Å) for ϵ Cha 13–17 and several *ROSAT* candidates during 2011 July 30–31. All the observations were taken and reduced as described in Murphy, Lawson & Bessell (2010, 2012). Briefly, we ran WiFeS in single-star mode with 2× spatial binning (1 arcsec spaxels) and used custom IRAF, FIGARO and PYTHON routines to extract, wavelength-calibrate

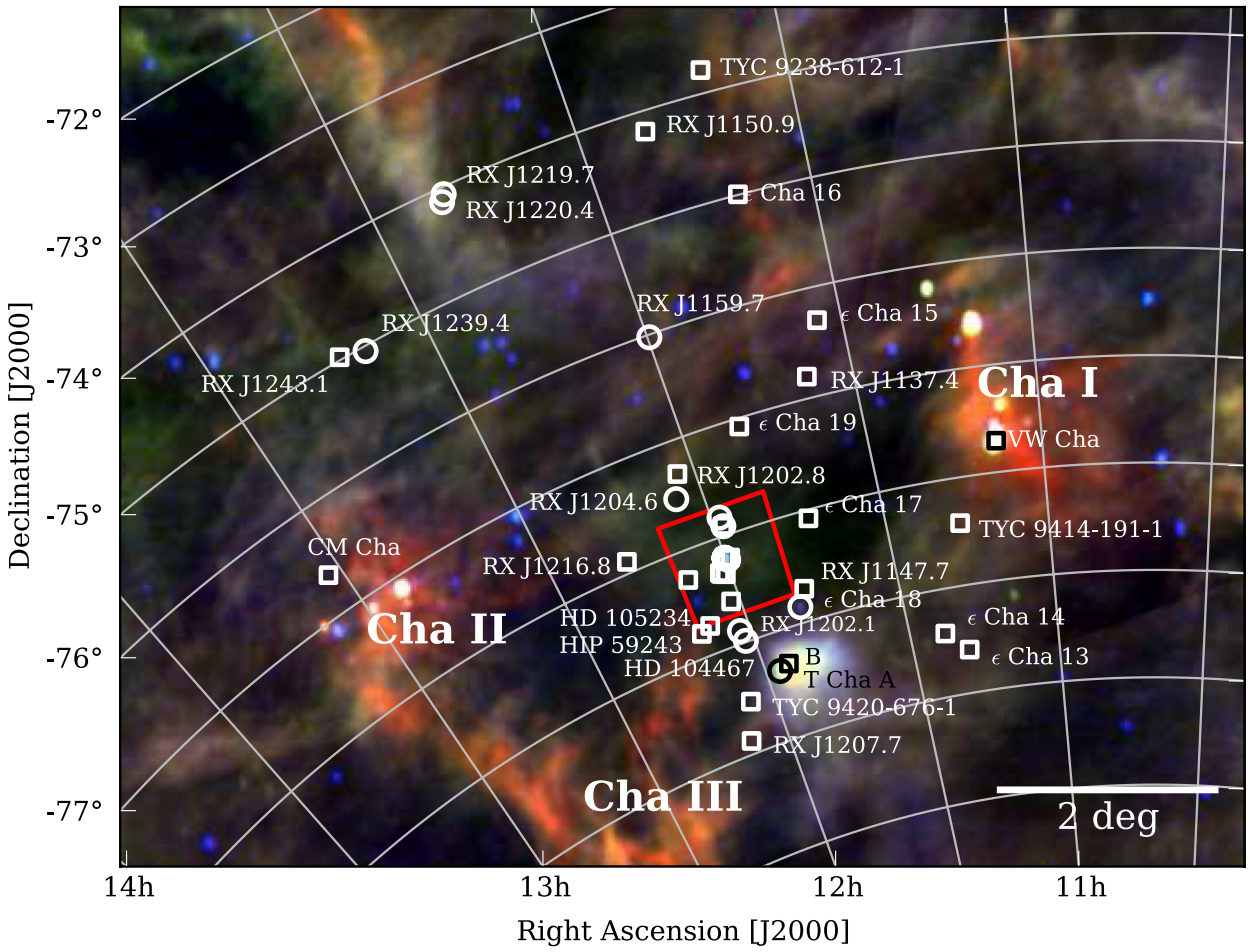

Figure 2. *Infrared Astronomical Satellite* (*IRAS*) 100 μm (red)/60 μm (green)/25 μm (blue) colour composite of the Chamaeleon region, with proposed ϵ Cha members from the literature (squares) and Torres et al. (2008) (circles). η Cha members in the Torres et al. solution, HD 82879, the likely AB Dor member HIP 55746 and several members north of $\delta = -72°$ are not shown (see Fig. 22). The red square shows the 1 deg^2 extent of Fig. 1.

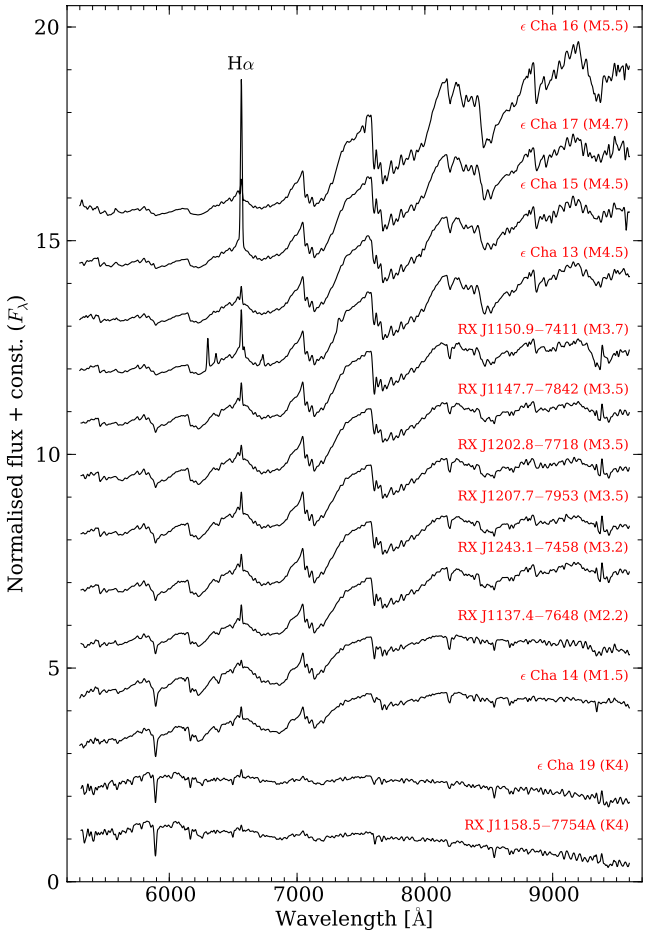

Figure 3. Flux-calibrated WiFeS/*R*3000 spectra of the low-mass candidates listed in Table 2. The spectra have been smoothed with a 10-px Gaussian kernel and normalized over the region 7400–7550 Å for display.

and combine the five image slices that contained the majority of the stellar flux. The *R*3000 spectra were corrected for telluric absorption and flux calibrated using contemporaneous observations of the white dwarf EG 131. We took arc frames after each *R*7000 exposure and radial velocities were calculated by cross-correlation of the spectra against 5–7 K and M-type standards observed each night.

The WiFeS/*R*3000 spectra are plotted in Fig. 3. RX J1137.4−7648 and RX J1147.7−7842 (Zuckerman & Song 2004) have no previously published spectroscopy. The former is a 3 arcsec approximately equal-brightness visual binary that was unresolved in the typical 2–2.5 arcsec seeing of the *R*3000 observations. During a night of exceptional $\lesssim$1 arcsec seeing on 2011 May 16, we resolved the pair and extracted minimally blended *R*7000 spectra. A full listing of WiFeS spectral types, Li I λ6708 and Hα equivalent widths (EWs) and mean radial velocities are given in Table 2. 15 candidates have no previous velocity measurement.

3.2 Spectral types and reddening

We determined the spectral types in Table 2 using a selection of molecular indices from Riddick, Roche & Lucas (2007) and visual comparison to η and ϵ Cha spectra from Lyo, Lawson & Bessell (2004b, 2008) and the Pickles (1998) library. The average WiFeS/*R*3000 values agree with those previously determined at the 0.1–0.3 subtype level.

There is evidence for a small amount of reddening between the Sun and the Chamaeleon cloud complex (Knude & Hog 1998). Compared to (unreddened) η Cha spectra, we estimate the WiFeS spectrum of 2MASS J11334926−7618399 (ϵ Cha 15) is reddened by $E(B-V) \approx 0.15$ mag, while 2MASS J11432669−7804454 (ϵ Cha 17) and RX J1243.1−7458 are reddened by no more than 0.1 mag. With the exception of VW Cha (Cha I member?) and T Cha AB (possibly associated with the dark cloud Dcld 300.2−16.9; Nehmé et al. 2008) the other candidates lie in regions of low-intensity dust emission (see Fig. 2). This is also apparent in the

Table 2. WiFeS observations of ϵ Cha candidates from the literature.

ID	Name	Spectral[a] type	$E(B-V)$[a] (mag)	Li I EW (±50 mÅ)	RV (km s^{-1})	σ_{RV}^{c} (km s^{-1})	Hα EW (±1 Å)	N_{obs}	Δt (d)
13	2MASS J11183572−7935548	M4.5	0	600	19.3[b]	1.6[b]	[−30, −18]	7	477
14	RX J1123.2−7924	M1.5	0	150	2.7[b]	2.9[b]	−2	6	477
15	2MASS J11334926−7618399	M4.5	0.15	650	16.7[b]	1.5[b]	−6	5	413
	RX J1137.4−7648	M2.2	0	0	∼14	–	−1.5	1	–
16	2MASS J11404967−7459394	M5.5	0	700	10.3	1.0	[−35, −11]	4	411
17	2MASS J11432669−7804454	M4.7	<0.1	700	15.6	1.0	[−120, −60]	6	480
	RX J1147.7−7842	M3.5	0	650	16.1	0.9	[−7, −4]	5	409
19	RX J1150.4−7704	K4	0	500	6.1[b]	1.6[b]	−1	5	479
	RX J1150.9−7411	M3.7	0	500	15.0	1.2	−8	4	59
21	RX J1158.5−7754A	K4	0	500	19.9	0.8	−0.5	4	480
1	CXOU J115908.2−781232	–	–	650	15.1	0.2	−5	3	356
10	2MASS J12005517−7820296	–	–	600	10.7[b]	1.3[b]	[−20, −10]	6	411
11	2MASS J12014343−7835472	–	–	700	20.0	0.6	[−140, −70]	3	370
8	USNO-B 120144.7−781926	–	–	500	14.9	1.1	[−45, −20]	4	60
9	CXOU J120152.8−781840	–	–	650	16.5	1.1	−8	4	411
	RX J1202.8−7718	M3.5	0	300	17.1	1.2	[−12, −5]	4	411
12	2MASS J12074597−7816064	–	–	500	15.4[b]	2.3[b]	−3.5	5	410
	RX J1207.7−7953	M3.5	0	550	15.0	0.7	−4	4	414
	RX J1243.1−7458	M3.2	<0.1	600	13.5	0.7	[−7, −4]	4	60

[a]Spectral types and reddening values determined from WiFeS *R*3000 spectra.
[b]WiFeS *R*7000 time series shows a velocity trend indicative of binarity (see Section 4.2.1 and Table 5).
[c]Standard error of the mean, $\sigma_{RV} = \sigma/\sqrt{N_{obs}}$.

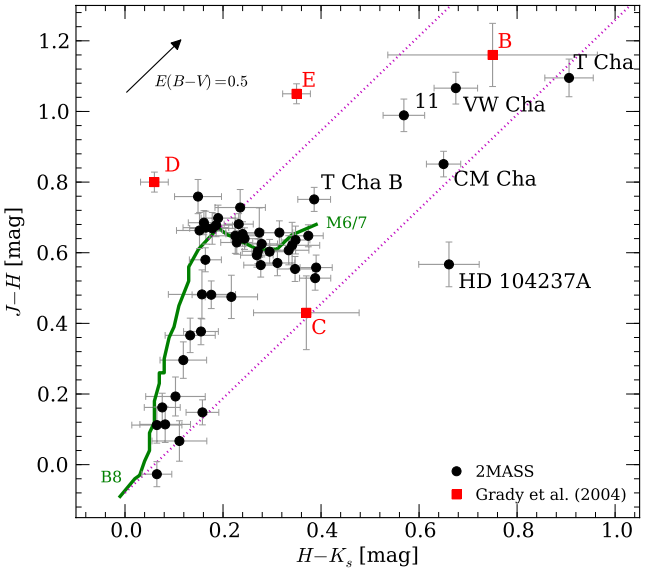

Figure 4. 2MASS two-colour diagram for ϵ Cha candidates (black circles), with VLT/NACO photometry for HD 104237B–E from Grady et al. (2004) (red squares) and the main-sequence colours of Kraus & Hillenbrand (2007, solid line). The Schlegel, Finkbeiner & Davis (1998) reddening vector (arrow, dotted lines) was transformed to the 2MASS system using the relations of Carpenter (2001). The position of HD 104237D blueward of the locus of reddened stars is due to photometric errors (Grady et al. 2004).

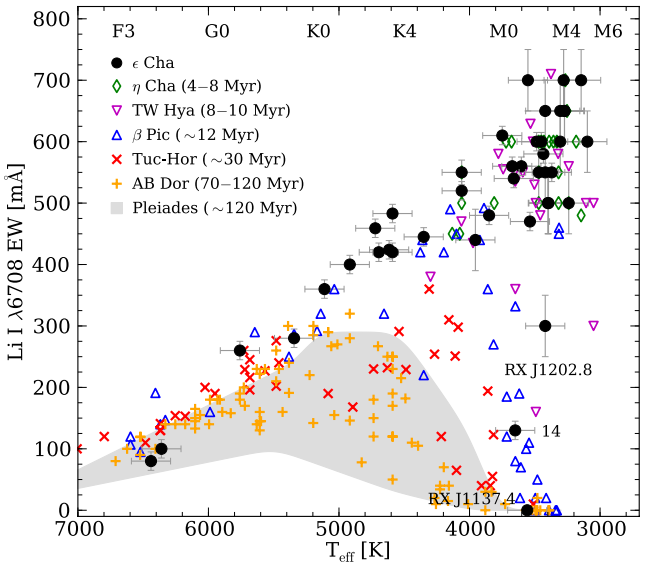

Figure 5. Li I λ6708 EWs for ϵ Cha candidates (black points, with errors), compared to members of young, nearby associations from da Silva et al. (2009). Members of the η Cha open cluster and the envelope of EWs observed in the Pleiades are also plotted. Following da Silva et al., effective temperatures were calculated from the spectral-type $T_{\rm eff}$ relation of Kenyon & Hartmann (1995).

2MASS two-colour diagram (Fig. 4), where all but a handful of stars follow the zero-reddening locus. To supplement the WiFeS observations, we estimated reddenings for all candidates using Fig. 4 and literature spectral types and photometry. The adopted values are given in Table B1. An optically thick circumstellar disc may also contribute to excess near-infrared (NIR) emission. Several of the stars in the top-right corner of Fig. 4 host such discs (see Section 6.3).

3.3 Lithium depletion

The amount of photospheric lithium depletion observed in low-mass stars can serve as a mass-dependent clock over pre-main-sequence time-scales (e.g. Mentuch et al. 2008; da Silva et al. 2009). We plot in Fig. 5 the distribution of Li I λ6708 EWs assembled from the literature and WiFeS observations. The latter were obtained by fitting Gaussian line profiles, with the 50 mÅ error estimated from multiple observations and by varying the integration limits. No attempt was made to correct for contamination by the weak Fe I line at 6707.4 Å (Soderblom et al. 1993) as its effect is negligible at these large EWs. We also see no evidence of strong continuum veiling, unsurprising given the low accretion rates (see Section 6.3.3). The individual measurements and their sources are listed in Table B1. Seven stars have no lithium measurements. Two are A-type stars which are not expected to show Li I λ6708 absorption and the rest have no available spectra.

We also plot in Fig. 5 Li I λ6708 EW values of young association members from da Silva et al. (2009). The sensitivity of lithium depletion to both stellar age and mass is evident in the older groups. Several late-type members of TW Hya show significant depletion and the slightly older β Pic (∼12 Myr) presents a steep decline down to its depletion boundary at a spectral type of ∼M4 (Song, Bessell & Zuckerman 2002). Assuming that the two ϵ Cha candidates at ∼3500 K with low EWs are true members provides an upper age limit of 8–10 Myr, the age of TW Hya. The non-detection of lithium in RX J1137.4−7648 implies it is at least as old as members of the Tucana–Horologium association (∼30 Myr). Both RX J1137.4−7648 and ϵ Cha 14 are also proper motion outliers (see next section). If these depleted stars are not members of ϵ Cha then the remaining late-type candidates have lithium measurements consistent with an age no older than the 4–8 Myr η Cha cluster.

4 KINEMATICS OF CANDIDATE MEMBERS

4.1 Proper motions

Nine stars have proper motions in the latest reduction of the *Hipparcos* catalogue (van Leeuwen 2007) and a further 10 were recovered in Tycho-2 (Høg et al. 2000). We adopted these proper motions in the kinematic analysis of Section 5 with the exception of T Cha, which has a large error in *Hipparcos* and is not in Tycho-2. For this star, we used the higher precision value from Southern Proper Motion (SPM4), the fourth iteration of Yale/San Juan Southern Proper Motion Catalog (Girard et al. 2011). SPM4 contains absolute proper motions for over 103 million objects, including nearly all (49/52) of the proposed ϵ Cha members. Only HD 104237B/C and 2MASS J12014343−7835472 (underluminous due to an edge-on disc; Luhman 2004b) were not found in SPM4. To check for discordant proper motions, we also queried the recent UCAC4 (Zacharias et al. 2013) and PPMXL (Röser, Demleitner & Schilbach 2010) catalogues but UCAC4 gave fewer matches (43/52) and in general PPMXL has less precise astrometry (also see discussion in Girard et al. 2011). The results of these cross-matches are summarized in Fig. 6. Proper motions from SPM4 and UCAC4 are somewhat correlated as they share some first epoch astrograph data (Zacharias et al. 2013). As expected, the majority of stars cluster around the projection of the ϵ Cha space motion on the sky at 100–120 pc. However, there are several stars with proper motions far from those expected of members.

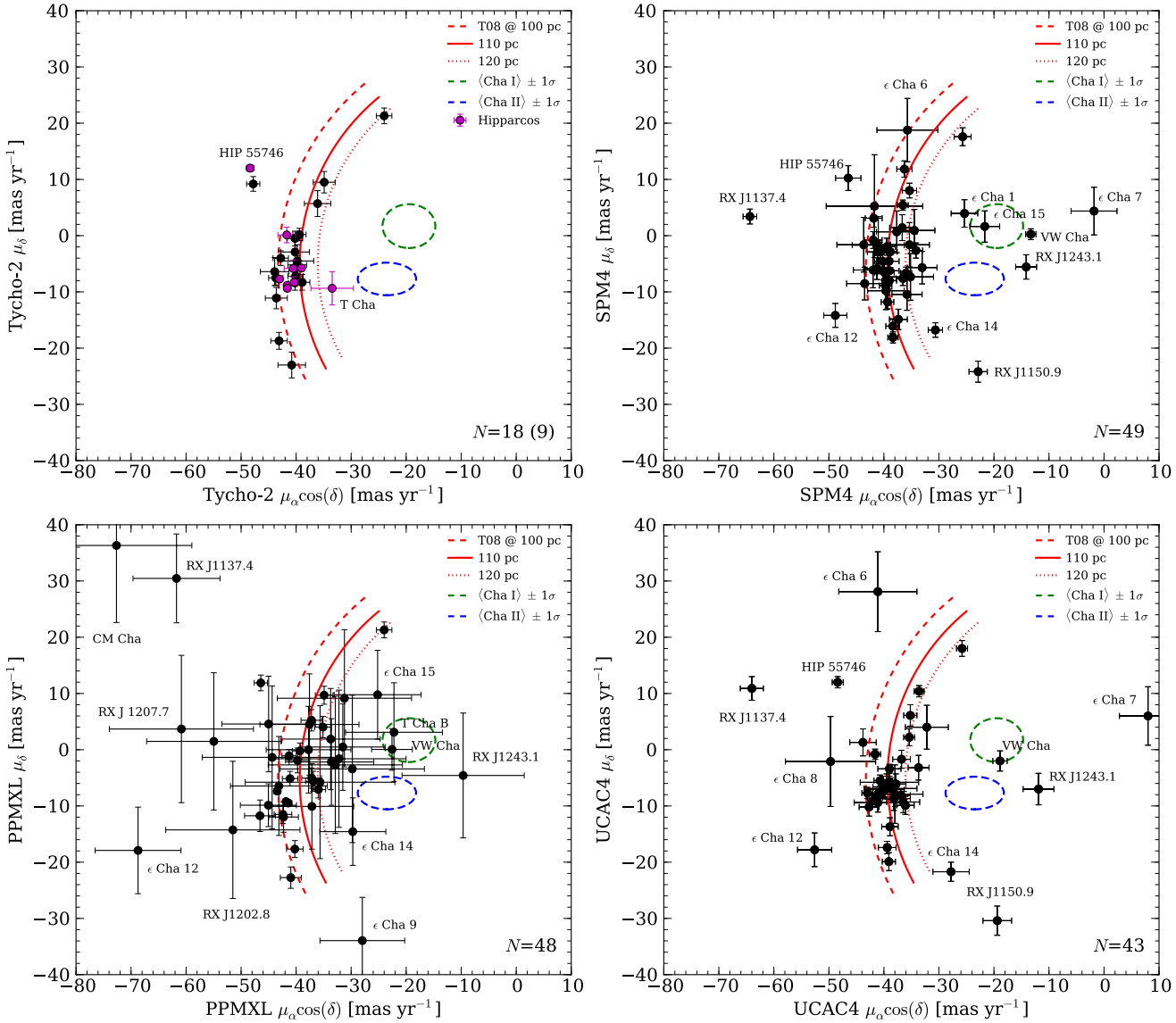

Figure 6. Proper motions of candidates in the *Hipparcos*/Tycho-2 (top left), SPM4 (top right), PPMXL (bottom left) and UCAC4 (bottom right) catalogues. The number of matches is given in the corner of each panel. The red lines show the Torres et al. (2008) space motion projected on to the sky at $\delta = -79^\circ$ and $130^\circ < \alpha < 210^\circ$ and distances of 100–120 pc. The green and blue ellipses are the mean proper motions of Cha I and II sources from Lopez Martí et al. (2013).

4.1.1 Outlying proper motions

HIP 55746 was reclassified as a member of the AB Doradus association by Torres et al. (2008); its *Hipparcos* proper motion and parallax are consistent with this new classification. Spectroscopically older RX J1137.4−7648 is likely a nearby, unrelated system. CXOU J120152.8−781840 (ϵ Cha 9) and 2MASS J12074597−7816064 (ϵ Cha 12) were noted by Fang et al. (2013) as having outlying PPMXL proper motions. With new UCAC4 and SPM4 astrometry, only ϵ Cha 12 remains an outlier. We observed large (∼13 km s^{-1}) radial velocity shifts (see Section 4.2) in the star which may indicate the presence of an unseen companion affecting the proper motion. RX J1123.2−7924 (ϵ Cha 14) is also suspected of having a close companion, though its lithium depletion implies an age older than ϵ Cha. RX J1150.9−7411 has a confirmed close companion (Köhler 2001) which may have altered its proper motion. Terranegra et al. (1999) found RX J1243.1−7458 was a kinematic but not spatial outlier to their proposed moving group. Its proper motion is near the mean of Cha II cloud members. VW Cha, CXOU J115908.2−781232 (ϵ Cha 1) and 2MASS J11334926−7618399 (ϵ Cha 15) may similarly be associated with the Cha I cloud. HD 104237D and E (ϵ Cha 6 and 7) are probably affected by their location close to HD 104237A.

4.1.2 Discordant proper motions

After comparing SPM4 and UCAC4, there were four stars with proper motions that differed by more than 2σ in either component. Their astrometry is collated in Table 3, with values from PPMXL for comparison. Terranegra et al. (1999) and Ducourant et al. (2005) calculated proper motions for 15 and 20 of the candidates, respectively. Because of their different source observations these studies provide an independent check on the SPM4 measurements. The four stars whose proper motions disagreed with SPM4 by more than 2σ are listed in Table 4.

The Ducourant et al. proper motion for VW Cha agrees with both UCAC4 and PPMXL. We adopted the UCAC4 value, while

Table 3. Candidates whose SPM4 and UCAC4 proper motions disagree by more than 2σ.

Name	SPM4 (mas yr^{-1})		UCAC4 (mas yr^{-1})		PPMXL (mas yr^{-1})	
	$\mu_\alpha \cos\delta$	μ_δ	$\mu_\alpha \cos\delta$	μ_δ	$\mu_\alpha \cos\delta$	μ_δ
VW Cha	-13.3 ± 0.9	$+0.3 \pm 1.0$	-18.9 ± 1.3	-2.0 ± 1.8	-22.6 ± 3.7	$+0.1 \pm 3.7$
RX J1123.2−7924 (ϵ Cha 14)	-30.6 ± 1.3	-16.8 ± 1.3	-27.8 ± 3.3	-21.7 ± 1.7	-29.7 ± 6.0	-14.6 ± 6.0
RX J1137.4−7648	-64.4 ± 1.2	$+3.4 \pm 1.3$	-64.0 ± 2.1	$+10.9 \pm 2.1$	-61.7 ± 7.9	$+30.5 \pm 7.9$
CM Cha	-33.1 ± 2.7	-5.7 ± 2.9	-32.2 ± 3.9	$+4.0 \pm 3.9$	-72.7 ± 13.7	$+36.3 \pm 13.7$

Table 4. Candidates whose Ducourant et al. (2005) or Terranegra et al. (1999) proper motions disagree with SPM4 by more than 2σ.

Name	SPM4 (mas yr^{-1})		Ducourant et al. (2005) (mas yr^{-1})		Terranegra et al. (1999) (mas yr^{-1})	
	$\mu_\alpha \cos\delta$	μ_δ	$\mu_\alpha \cos\delta$	μ_δ	$\mu_\alpha \cos\delta$	μ_δ
VW Cha	-13.3 ± 0.9	$+0.3 \pm 1.0$	-24 ± 3	$+2 \pm 3$	–	–
RX J1150.9−7411	-22.9 ± 1.7	-24.2 ± 1.9	$+15 \pm 16$	$+37 \pm 16$	-39.0 ± 4.2	$+4.4 \pm 2.9$
RXJ1219.7−7403	-39.0 ± 1.3	-8.0 ± 1.5	-37 ± 11	-15 ± 11	-40.4 ± 6.9	-2.8 ± 0.2
CM Cha	-33.1 ± 2.7	-5.7 ± 2.9	-66 ± 12	$+23 \pm 12$	–	–

for RX J1123.2−7924 (ϵ Cha 14), RX J1219.7−7403 and RX J1137.4−7648 we retained the SPM4 proper motions. CM Cha is a special case. Although the Ducourant et al. proper motion matches PPMXL within the (large) errors, we have adopted the higher precision SPM4 values. If the larger proper motion is correct then CM Cha may be even closer to the Sun than ϵ Cha (see discussion in Lopez Martí et al. 2013). The motion of RX J1150.9−7411 measured by both studies differs significantly from SPM4 and UCAC4. While Ducourant et al. used an incorrect position from Alcala et al. (1995) and gave the proper motion of an unrelated star, the Terranegra et al. proper motion for RX J1150.9−7411 is very close to other candidates. We chose this value over SPM4 but note that it may be influenced by a close companion (Köhler 2001). The proper motions of all stars and their sources are listed in Table B1.

4.2 Radial velocities

Candidate radial velocities from our WiFeS observations and the literature are listed in Table B1. For 2MASS J11550485−7919108 (T Cha B), we adopted the value for T Cha itself, $14.0 \pm 1.3\,\mathrm{km\,s^{-1}}$ (Guenther et al. 2007). Since T Cha exhibits large ($\Delta RV \sim 10\,\mathrm{km\,s^{-1}}$) aperiodic velocity variations on daily timescales (Schisano et al. 2009), we caution that this velocity may not be representative. However, it agrees with velocities reported by Torres et al. (2006) ($16.3 \pm 5.8\,\mathrm{km\,s^{-1}}$) and Franchini et al. (1992) ($14.6 \pm 2.1\,\mathrm{km\,s^{-1}}$). For HD 104237E ($\epsilon$ Cha 7), we adopted the velocity of the *D* component (ϵ Cha 6), $13.4\,\mathrm{km\,s^{-1}}$. Grady et al. (2004) stated that both stars were a good velocity match to HD 104237A ($14\,\mathrm{km\,s^{-1}}$), although they did not explicitly give a velocity for the *E* component.

4.2.1 Spectroscopic binaries

The multi-epoch WiFeS observations revealed six candidates (marked in Table 2) with velocity variations indicative of binarity. Two more candidates, RX J1158.5−7754A (ϵ Cha 21) and RX J1243.1−7458, have mean velocities that differ significantly from those in the literature. The velocities of these eight stars are presented in Table 5. The individual errors in the table are the standard deviations of cross-correlations against 4–8 K and M-type standards observed each night. We also found that the Torres et al. (2008) members RX J1202.1−7853 and RX J1220.4−7407 have velocities in Guenther et al. (2007) and Covino et al. (1997) that differ outside their errors. These stars are also listed in Table 5.

Köhler (2001) conducted a speckle and direct-imaging survey for close (0.13–6 arcsec) companions around 82 *ROSAT* sources in Chamaeleon, including six of the candidates in Table 5. We confirm the binarity of RX J1158.5−7754A (ϵ Cha 21), RX J1243.1−7458 and RX J1220.4−7407. Köhler (2001) also found close companions around HIP 55746 (probable AB Dor member) and RX J1150.9−7411. Four WiFeS measurements of this star over 59 d showed no significant velocity variation, unsurprising given the cadence of the observations. Despite finding no close companions around RX J1123.2−7924 (ϵ Cha 14), the star is clearly a spectroscopic binary. We have also confirmed suspicions about the binarity of RX J1150.4−7704 (ϵ Cha 19) raised by Covino et al. (1997), with both our WiFeS time series and an earlier measurement by Guenther et al. (2007) showing a clear velocity variation. With only two measurements we cannot confirm the spectroscopic binarity of RX J1202.1−7853, though the large velocity difference ($12.1 \pm 2\,\mathrm{km\,s^{-1}}$) is compelling.

4.2.2 Other known or suspected binaries

RX J1204.6−7731 is a double-lined spectroscopic binary (Torres et al. 2008) and HD 104467 is a suspected single-line system (Cutispoto et al. 2002). RX J1137.4−7648 and ϵ Cha are approximately equal-brightness visual binaries and VW Cha is a hierarchical triple (Correia et al. 2006). Böhm et al. (2004) detected a 1.7 $M_\odot$ companion to HD 104237A in an eccentric 19.8 d orbit (separation ∼0.1 au) which they called HD 104237b. It is likely the source of the late-type spectral features in HD 104237A reported by Feigelson et al. (2003) and is distinct from HD 104237B, which is resolved at ∼150 au (1.3 arcsec).

5 KINEMATIC MEMBERSHIP ANALYSIS

5.1 Initial observational isochrone

To compare the candidates' photometry to kinematic distances derived in Section 5.2 an absolute isochrone is required. We plot in Fig. 7, extinction-corrected DENIS (Epchtein et al. 1999) and 2MASS (Skrutskie et al. 2006) photometry with 3 and 5 Myr isochrones from Dotter et al. (2008) and Siess, Dufour & Forestini

Table 5. Candidates suspected of spectroscopic binarity.

Star Epoch	RV (km s^{-1})	σ(RV) (km s^{-1})	Köhler (2001) companion?
2MASS J12005517−7820296 (ϵ Cha 10)			–
2010 May 04	+15.0	1.1	
2011 Jan 09	+7.2	0.8	
2011 Feb 24	+9.0	2.0	
2011 May 09	+13.4	1.1	
2011 May 17	+12.0	1.7	
2011 Jun 19	+7.5	1.0	
2MASS J12074597−7816064 (ϵ Cha 12)			–
2010 May 05	+23.4	1.5	
2011 Jan 08	+10.7	0.8	
2011 Jan 13	+15.2	1.9	
2011 May 17	+16.7	1.1	
2011 Jun 19	+11.0	0.5	
2MASS J11183572−7935548 (ϵ Cha 13)			–
2010 Feb 25	+19.8	2.6	
2010 May 02	+15.8	0.5	
2010 Dec 20	+14.3	1.9	
2011 Feb 11	+17.9	1.2	
2011 Feb 12	+17.8	2.5	
2011 May 16	+26.7	1.2	
2011 Jun 17	+23.2	2.7	
RX J1123.2−7924 (ϵ Cha 14)			N (#42)
2010 Feb 25	−2.6	3.1	
2010 May 02	−5.0	0.1	
2010 Dec 20	−0.4	1.7	
2011 Feb 10	+2.4	0.4	
2011 May 16	+7.3	1.8	
2011 Jun 17	+14.1	2.1	
Covino et al. (1997)	+10.0	2.0	
2MASS J11334926−7618399 (ϵ Cha 15)			–
2010 May 02	+13.9	0.6	
2010 Dec 20	+14.0	1.5	
2011 Feb 11	+15.1	0.7	
2011 May 16	+20.4	1.5	
2011 Jun 19	+20.1	0.6	
RX J1150.4−7704 (ϵ Cha 19)			N (#47)
2010 Feb 25	+9.0	3.5	
2010 May 06	+9.7	1.7	
2011 Feb 10	+6.2	0.4	
2011 May 17	+1.0	1.7	
2011 Jun 19	+4.5	1.4	
Covino et al. (1997)	SB?		
Guenther et al. (2007)	−3.3	1.0	
RX J1158.5−7754A (ϵ Cha 21)			Y (#50, 0.07 arcsec)
2010 Feb–2011 Jun	+19.9	0.8	
Covino et al. (1997)	+13.1	2.0	
James et al. (2006)	+10.2	–	
RX J1243.1−7458			Y (#73, 0.3 arcsec)
2011 Apr–Jun	+13.5	0.7	
Covino et al. (1997)	+7.0	2.0	
RX J1202.1−7853			N (#55)
Guenther et al. (2007)	+17.1	0.2	
Covino et al. (1997)	+5	2	
RX J1220.4−7407			Y (#65, 0.3 arcsec)
Guenther et al. (2007)	+12.3	0.4	
Covino et al. (1997)	+18	2	

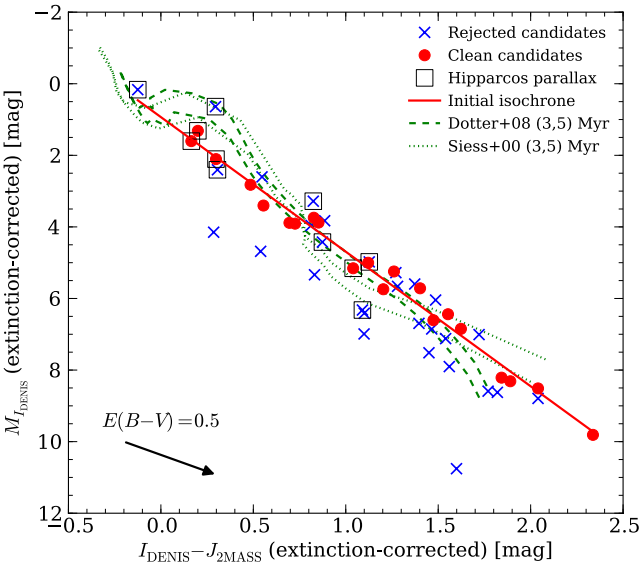

Figure 7. The initial isochrone (solid line) used in the kinematic analysis. A linear fit was performed on the extinction-corrected photometry (red circles) after excluding binaries, proper motion and Li I outliers and NIR excess sources (blue crosses). Siess et al. (2000) (dotted lines) and Dotter et al. (2008) (dashed lines) theoretical isochrones are shown for comparison.

(2000). Stars without *Hipparcos* parallaxes were assigned a distance of 110 pc and we adopted the reddening relations $A_I = 0.601A_V$ and $A_{I-J} = 0.325A_V$ from Schlegel et al. (1998). There is significant variation between the observed photometry and the isochrones, and also between different model sets. Rather than using a theoretical isochrone, which would require assuming an age and could introduce model-dependent photometric distances, we adopted a similar strategy to Torres et al. (2006) and used the candidates themselves to define an ad hoc, empirical isochrone. After excluding known or suspected binaries, proper motion outliers and those stars with 2MASS colour excesses or low Li I λ6708 EWs, the 21 remaining candidates were well fitted by the linear regression:

$$M_I = 3.760 \times (I - J) + 0.93 \quad (1)$$

This relation was used in the kinematic analysis in the next section. As noted by Torres et al. (2006), defining an isochrone assuming membership in a group then using it to test membership appears to be circular reasoning. However, the high-quality candidates used to define equation (1) all have photometry, proper motions, radial velocities and lithium measurements consistent with membership in ϵ Cha and are highly likely to represent the true association isochrone. Moreover, several stars have *Hipparcos* parallaxes which anchor the distance scale of the fainter candidates.

Although binaries were not included in the calculation of equation (1), before running the kinematic analysis we corrected the photometry of RX J1150.9−7411, RX J1158.5−7754A (ϵ Cha 21), RX J1220.4−7407, RX J1243.1−7458, HIP 55746, ϵ Cha and VW Cha to that of the primary using published flux ratios. For RX J1137.4−7648, we assumed an equal-mass system. More details and *IJHK*$_s$ photometry for all candidates is given in Table B2.

5.2 Member selection

With the best-available proper motions, velocities and photometry we tested membership of the candidates using a similar technique

Table 6. Heliocentric velocities and positions of η and ϵ Chamaeleontis.

–	U	σ_U	V	σ_U	W	σ_W	X	σ_X	Y	σ_Y	Z	σ_Z
			(km s^{-1})						(pc)			
ϵ Cha (this work)	−10.9	0.8	−20.4	1.3	−9.9	1.4	54	3	−92	6	−26	7
Torres et al. (2008)	−11.0	1.2	−19.9	1.2	−10.4	1.6	50	–	−92	–	−28	–
η Cha (updated)[a]	−10.2	0.2	−20.7	0.1	−11.2	0.1	33.4	0.4	−81.0	1.0	−34.9	0.4

[a]Derived from the weighted mean *Hipparcos*/Tycho-2 positions and proper motions of η Cha, RS Cha, RECX 1 and HD 75505 ($08^h40^m48\overset{s}{.}24$, $-79°00'24.8''$; $\mu_\alpha \cos\delta = -29.35 \pm 0.13$ mas yr^{-1}, $\mu_\delta = 27.41 \pm 0.13$ mas yr^{-1}), the weighted mean *Hipparcos* parallaxes of η Cha and RS Cha (94.3 ± 1.1 pc; van Leeuwen 2007) and the weighted mean radial velocities of RECX 1,3,4–6,9,10–13 (18.3 ± 0.1 km s^{-1}; Brandeker, private communication).

to the convergence method of Torres et al. (2006, 2008). First, for each star without a good *Hipparcos* parallax[3] we found the distance which minimized the difference in space motions:

$$K = \sqrt{(U - U_0)^2 + (V - V_0)^2 + (W - W_0)^2}, \quad (2)$$

where $K = K(\alpha, \delta, \mu_\alpha, \mu_\delta, RV; d)$ and (U_0, V_0, W_0) is the mean space motion (initially from Torres et al. 2008).[4] With this *kinematic* distance (or a parallax) and the extinction-corrected photometry we then calculated the difference in absolute magnitude (ΔM_I) between the star and the isochrone (equation 1). Candidates were retained as possible members if $K < 3.5$ km s^{-1} (a difference of 2 km s^{-1} in each dimension and similar to the observed velocity dispersion in young groups) and $|\Delta M_I| < 1$ mag (the approximate rms variation around the initial isochrone). To exclude background members of Cha I and II, we additionally required $d < 150$ pc. From these kinematic members a new isochrone and (U_0, V_0, W_0) were calculated. The process was iterated until the membership and space motion no longer changed significantly.

Due to the high-quality initial space motion from Torres et al. (2008) the final list of 25 kinematic members converged on the second iteration while final distances and velocities took four iterations (for $\Delta d = 1$ pc). Both the mean space motion (Table 6) and distance (110 ± 7 pc) agree with those previously determined by Torres et al. (2008). The revised values should be more accurate as they were derived from a larger number of members and by not subsuming η Cha into the ϵ Cha solution.

Fig. 8 shows the final distribution of K and ΔM_I values. There are several candidates with $|\Delta M_I| < 1$ mag but velocity differences in excess of the 3.5 km s^{-1} limit. To account for non-systemic radial velocities and the lower resolution WiFeS observations we selected as *a posteriori* kinematic members those candidates with $K < 8$ km s^{-1}. The mean space motion and isochrone were *not* updated after this step. Six of the eight stars this criterion added are known or suspected spectroscopic binaries. The four candidates with $K > 8$ km s^{-1} are either members with obviously erroneous proper motions (ϵ Cha 6 and 7) or underluminous spectroscopic binaries (ϵ Cha 14 and 19). Placing them near the isochrone would require unrealistic distances of 170–220 pc. ϵ Cha 14 also has a low (130 mÅ) lithium measurement. The three rejected candidates inside the shaded region have estimated distances greater than 150 pc. Fig. 9 presents the new ϵ Cha CMD and the twelve candidates rejected by our technique. As expected of true members, the tight clustering of *kinematic* distances in the CMD almost perfectly replicates the mean photometric isochrone of equation (1).

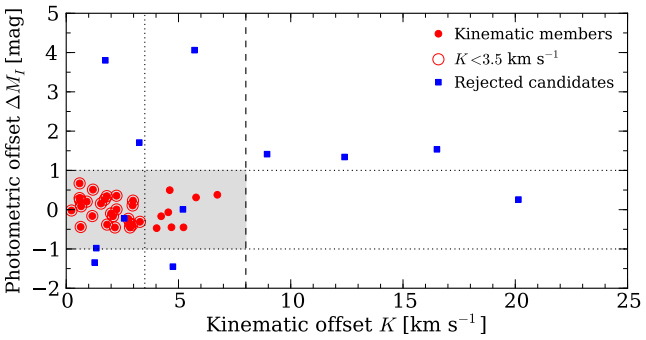

Figure 8. Results of the convergent analysis, showing the difference in space motions (K) and the offset from the final isochrone (ΔM_I). Dotted lines mark the ±1 mag and 3.5 km s^{-1} limits for calculating the association space motion (open circles), while the dashed line is the limit for selecting final kinematic members (filled circles).

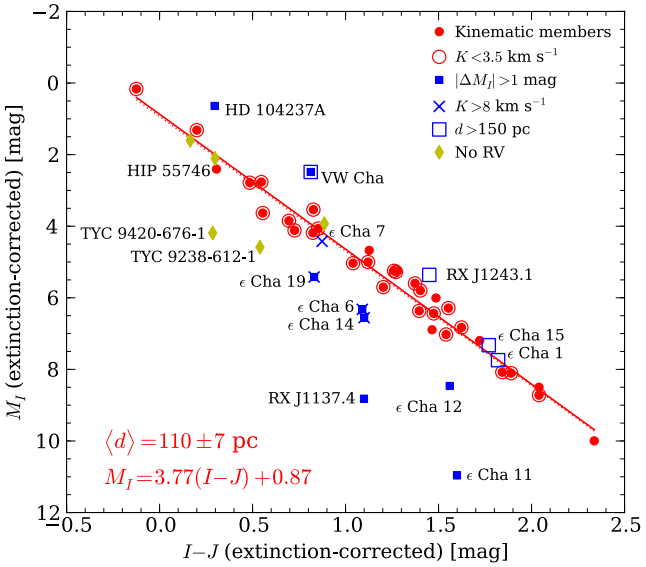

Figure 9. Colour–magnitude diagram of ϵ Cha after the membership analysis. Candidates rejected in the analysis are labelled (blue squares, crosses). ϵ Cha 11, HD 104237A and its companions ϵ Cha 6 and 7 are confirmed members with bad photometry or astrometry (see Appendix A). The five stars without radial velocities (yellow diamonds) are plotted at their best-fitting kinematic distance or *Hipparcos* parallax, if available.

Kinematic distances for those candidates observed by *Hipparcos* are compared to their trigonometric parallaxes in Fig. 10. All agree

[3] For *Hipparcos* candidates with a parallax error greater than 10 per cent, we adopted the kinematic distance in lieu of the trigonometric.

[4] Throughout this work, (U, V, W) are a right-handed triad with U (and X) increasing towards the Galactic Centre.

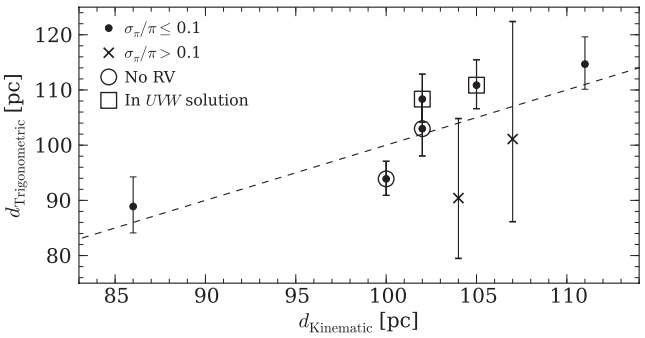

Figure 10. Comparison of trigonometric and kinematic distances. Kinematic distances for those stars without radial velocities were estimated from proper motions alone. The dashed line is the 1:1 relation. T Cha (relative parallax error ∼50 per cent) is not plotted.

within the 2σ errors. Only two parallaxes (ϵ Cha, HD 104036) were used in the final space motion solution. The other candidates had large parallax errors (in which case the kinematic distance was adopted) or failed one of the selection criteria.

6 RESULTS

6.1 Final membership of ϵ Cha

After considering the results of the kinematic, CMD and lithium analysis, our final membership for ϵ Cha contains 35 stars; 29 from the kinematic solution plus 2MASS J12014343−7835472 (ϵ Cha 11) and HD 104237A–E. The heliocentric positions and velocities of these stars are plotted in Fig. 11 and listed in Table 7. Six candidates (two selected as kinematic members) are provisional members requiring further observation. They are also plotted in Fig. 11 and listed in Table 8. The 11 stars unlikely to be members of ϵ Cha (two initially selected as kinematic members) are summarized in Table 9 with their suggested membership assignments. All of the provisional and non-members are discussed in greater detail in Appendix A, with several noteworthy confirmed members from Table 7.

6.2 Age of ϵ Cha

Fig. 12 shows the Hertzsprung-Russell Diagram (HRD) for confirmed and provisional members of ϵ Cha. The effective temperature of each star was obtained from its spectral type using the temperature scales of Kenyon & Hartmann (1995) for spectral types earlier than M1 and Luhman et al. (2003) for M1–M6. For TYC 9414-191-1, we adopted a spectral type of K5 ($A_V = 0.9$) which is consistent with its $B - V$ colour and position in Fig. 4. Luminosities were calculated using de-reddened J-band magnitudes and the bolometric corrections (BC) of Kenyon & Hartmann (1995). We adopted $M_{\rm bol,\odot} = 4.64$, appropriate for the Kenyon & Hartmann BC scale. Pre-main-sequence isochrones and evolutionary tracks from Dotter et al. (2008) are plotted for comparison.[5] The four early-type members fall around the 3–5 Myr isochrones, as do the majority of late-type stars. However, the solar-type members appear systematically older in this diagram, with ages of 5–10 Myr. Such mass-dependent age differences are unexpected and probably result from systematic errors in the models and/or temperature/luminosity scales.

Individual ages were obtained by interpolating the isochrones at the position of each star. The resulting age distribution is given in the top panel of Fig. 13. The median age of all members is $3.7^{+4.6}_{-1.4}$ Myr.[6] If we restrict the sample to $\log T_{\rm eff} < 3.65$ (K4 spectral type and later) to exclude the systematically older solar-type stars, the dispersion is much reduced and the median age is $3.2^{+2.4}_{-1.3}$ Myr. Excluding uncorrected binaries lowers the median low-mass age and dispersion by only 0.1 Myr. This age agrees with previous estimates using fewer stars (Fang et al. 2013) and different model grids (Feigelson et al. 2003; Luhman 2004b). Monte Carlo simulations along the 3 Myr model isochrone with realistic errors ($\sigma_{T_{\rm eff}} = 100$ K, $\sigma_{\log {\rm L/L}_\odot} = 0.05$) show that the observed dispersion around the median age is consistent with measurement errors alone, i.e. the low-mass members of ϵ Cha appear coeval.

As a comparison, we also calculated ages using the isochrones of Siess et al. (2000). The age distribution (Fig. 13, bottom panel) is very similar and both sets of models together indicate a median low-mass age of 3–5 Myr. This makes ϵ Cha one of the youngest groups in the solar neighbourhood ($\lesssim$150 pc) and its members ideal targets for high-sensitivity studies of young stars, discs and nascent planetary systems. Temperatures, luminosities and ages for all confirmed or provisional members are listed in Tables 7 and 8.

6.2.1 Age of η Cha

As they are commonly cited as being coeval (e.g. Torres et al. 2008), it is worthwhile to compare the ages of η and ϵ Cha. We conducted a similar analysis using the 18 core members of η Cha, adopting spectral types from Luhman & Steeghs (2004), a distance of 94 pc and correcting the photometry of the equal-mass binaries RECX 1, 9 and 12. The results suggest a small (1–3 Myr) age difference, with η Cha having median ages of $5.9^{+1.7}_{-2.4}$ (Dotter et al. 2008) and $7.1^{+1.4}_{-2.8}$ Myr (Siess et al. 2000). These agree with previous estimates (Lawson et al. 2001; Luhman & Steeghs 2004). A small age difference is also apparent in the CMD (Fig 14), where the sequence of single (or high mass-ratio binary) η Cha members lies slightly below the ϵ Cha sequence. Comparison against theoretical models again suggests an age difference of 1–3 Myr.

The strength of the Na I λ8183/8195 doublet is highly dependent on surface gravity in mid-to-late M-type stars. It can therefore be used as an age proxy for pre-main-sequence stars contracting towards their main-sequence radii. Lawson et al. (2009) used Na I strengths to rank the ages of several young associations. Their mean trends (Fig. 15) agree with the isochronal and lithium depletion age rankings of the groups. Furthermore, they resolved η and ϵ Cha in gravity, with the former appearing several Myr older. We computed the same Na I index after smoothing the WiFeS $R3000$ spectra to the $R \approx 800$ resolution of the Lawson et al. data and resampling to the same wavelength scale. Despite the large scatter, the revised ϵ Cha trend is still clearly younger than η Cha, confirming the previous HRD and CMD analyses.

[5] Although isochrones are only provided for $t > 250$ Myr, the tracks contain the full pre-main-sequence evolution. We created isochrones from 0.9 to 100 Myr ($\Delta \log t = 0.1$ Myr) by interpolating the tracks over 0.1–5 $M_\odot$.

[6] As a measure of dispersion, we adopted the 16th and 84th percentiles in the cumulative age distribution.

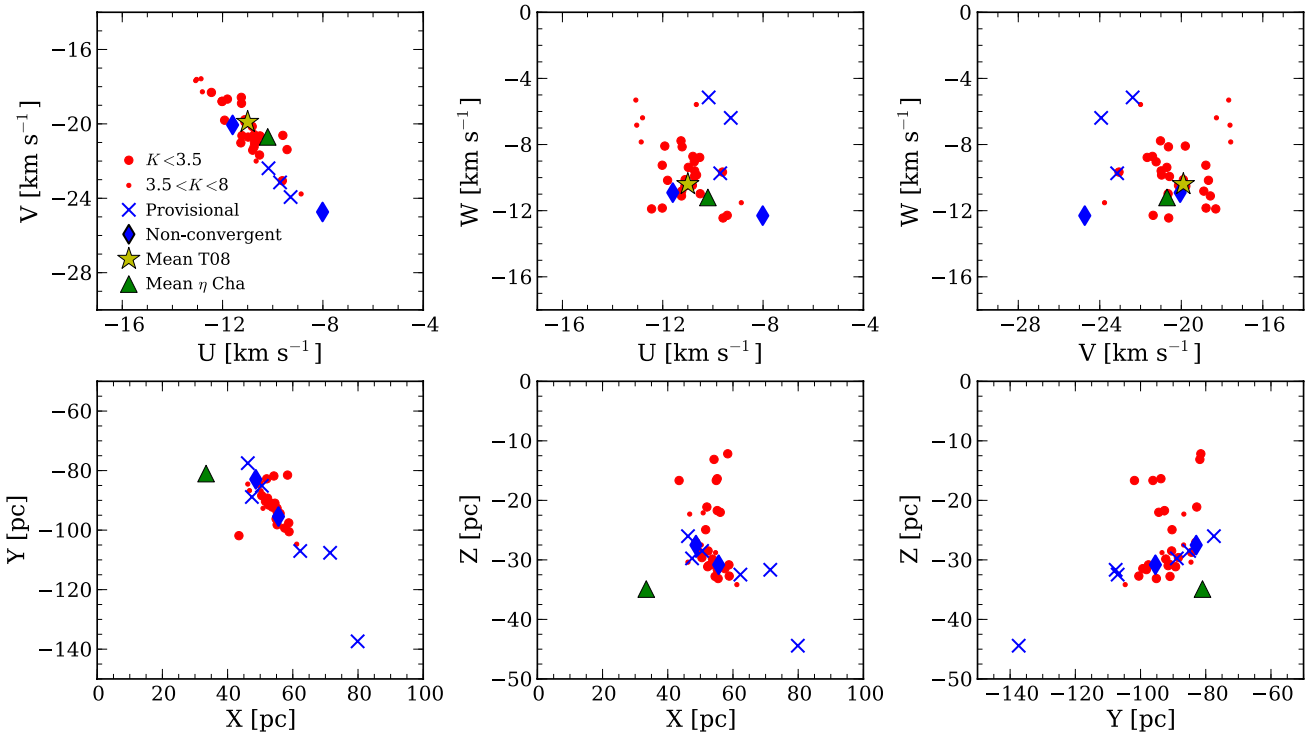

Figure 11. Heliocentric velocities and positions of kinematic members (red points), confirmed members not selected by the convergent analysis (HD 104237 and ϵ Cha 11; blue diamonds) and provisional candidates requiring confirmation (crosses). ϵ Cha 1 is shown at the 165 pc distance implied by its SPM4 proper motion. The previous Torres et al. (2008) and updated η Cha space motions are given by the yellow star and green triangle, respectively.

6.3 Circumstellar discs and accretion in ϵ Cha

To check for circumstellar disc emission, we queried the recent *Wide-field Infrared Survey Explorer* (*WISE*) All Sky Data Release (Wright et al. 2010). The components of HD 104237 were not resolved individually at the 6–12 arcsec resolution of *WISE*. Spectral energy distributions (SEDs) of the 13 members with excess emission at wavelengths shorter than 22 μm are plotted in Fig. 16. Also plotted is the SED of HD 104237E (ϵ Cha 7), which has a clear disc excess from 3 to 24 μm photometry reported by Grady et al. (2004) and Luhman et al. (2010). The former also reported strong excess K_s and L' emission from HD 104237B (ϵ Cha 4). The variety of SED morphologies in Fig. 16 is typical of rapidly evolving intermediate-age discs (Williams & Cieza 2011) and the manifold physical processes (photo-evaporation, accretion, grain growth, dynamical interactions with companions) shaping them. A similar range of discs are observed in η Cha (Sicilia-Aguilar et al. 2009). While a detailed analysis of the disc and dust properties of ϵ Cha members is outside the scope of this work, we briefly describe some germane results from the literature below.

Fang et al. (2013) presented *Spitzer Space Telescope* 7–35 μm spectroscopy of 10 members (ϵ Cha 1,2,5–12). Their spectrum of CXOU J115908.2−781232 (ϵ Cha 1) and preliminary *WISE* photometry showed no excess emission, whereas in the final *WISE* release there is a clear excess at 22 μm. USNO-B 120144.7−781926 (ϵ Cha 8) and 2MASS J12005517−7820296 (ϵ Cha 10) show signs of reduced disc heights due to dust settling and the disc around HD 104237E (ϵ Cha 7) may be undergoing partial dissipation in its inner regions, leaving the outer disc intact. Fang et al. attributed the underluminosity of 2MASS J12014343−7835472 (ϵ Cha 11) to a flared disc seen at moderately high inclination (∼85°), in which the central star is seen in only scattered light. 2MASS J11432669−7804454 (ϵ Cha 17) has a transitional disc with a strong 10 μm silicate feature (Manoj et al. 2011). The provisional member HD 105234 is surrounded by a warm, gas-poor debris disc (Currie et al. 2011). Unlike most debris discs it also has numerous solid-state features. MP Mus was classified by Mamajek, Meyer & Liebert (2002) as a 7–17 Myr old member of Lower Centaurus Crux (LCC) but its optically thick accretion disc is more consistent with the younger age of ϵ Cha. Such discs are rare around stars older than 5–10 Myr (see Section 6.3.1) and MP Mus was the only accretor with a *K*-band excess detected by that study from 110 solar-type members of Sco–Cen. The membership of this star is discussed in greater detail in Section 7.2.

Two candidates reclassified as Cha I members have infrared excesses. The SEDs of 2MASS J11334926−7618399 (ϵ Cha 15) and VW Cha are plotted in Fig. 16. We also constructed SEDs for the new halo members of η Cha (Murphy et al. 2010). The two members with detectable excesses are shown in Fig. 17.

6.3.1 *Circumstellar disc frequency*

Fang et al. (2013) reported a disc frequency of 55^{+13}_{-15} per cent (6/11) for the classical members (Feigelson et al. 2003; Luhman 2004b) in the core of ϵ Cha. Considering all 41 confirmed and provisional members there are 12 stars with excesses at wavelengths shorter than ∼8 μm (corresponding to the *Spitzer* IRAC bands). This yields a disc fraction of 29^{+8}_{-6} per cent.[7]

Based on the elevated disc fraction of ϵ Cha and other nearby groups, Fang et al. (2013) proposed that circumstellar disc evolution proceeds more slowly in sparse associations. We plot in Fig. 18 the

[7] Uncertainties for small samples are calculated for 68 per cent confidence intervals following the prescription of Cameron (2011).

Table 7. Confirmed members of the ϵ Cha association.

ID[a]	Name	Spectral type	Distance[b] (pc)	K^c	U	V	W	X	Y	Z	$T_{\rm eff}$	$L_{\rm bol}$	Age[d]
					(km s^{-1})				(pc)		(K)	($L_\odot$)	(Myr)
(22)	CP−68 1388	K1	112	2.2	−11.3	−21.0	−7.8	43.5	−101.9	−16.7	5080	1.4	7.9/13.2
13	2MASS J11183572−7935548	M4.5	101	4.2	−8.9	−23.8	−11.5	46.2	−84.5	−30.4	3198	0.084	2.5/4.4
16	2MASS J11404967−7459394	M5.5	101	5.8	−13.1	−17.7	−5.3	46.7	−86.7	−22.3	3058	0.011	13.8/–
17	2MASS J11432669−7804454	M4.7	117	1.7	−10.5	−21.7	−8.8	55.2	−98.2	−31.6	3169	0.041	5.7/–
(23)	RX J1147.7−7842	M3.5	106	2.9	−9.6	−20.6	−12.4	50.5	−88.4	−29.6	3343	0.24	0.9/2.2
18	RX J1149.8−7850	M0	110	1.8	−11.2	−18.9	−10.8	52.5	−91.5	−31.0	3850	0.44	2.1/2.9
(24)	RX J1150.9−7411	M3.7	108	4.6	−10.7	−22.0	−5.6	50.9	−92.7	−22.1	3314	0.092	3.9/5.2
(25)	2MASS J11550485−7919108	M3	115	1.8	−11.2	−20.6	−8.1	55.4	−95.1	−33.1	3415	0.092	6.6/6.6
(26)	T Cha	K0	108	0.9	−11.1	−19.8	−10.5	52.2	−89.2	−31.1	5250	1.2	12.7/20.7
20	RX J1158.5−7754B	M3	119	2.2	−11.3	−18.6	−11.1	57.5	−99.3	−31.5	3415	0.15	2.9/3.9
21	RX J1158.5−7754A	K4	104	4.7	−13.0	−17.6	−6.8	50.3	−86.8	−27.5	4590	0.75	7.2/–
(27)	HD 104036	A7	108H	3.3	−12.4	−18.3	−11.9	52.4	−90.5	−28.5	7850	20.0	2.8/7.2
2	ϵ Cha AB	B9	111H	2.8	−12.0	−18.8	−11.8	53.7	−92.3	−29.9	10500	99.9	2.6/2.8
(28)	RX J1159.7−7601	K4	107	0.6	−11.1	−19.9	−10.1	51.6	−90.3	−24.9	4590	0.50	14.3/14.4
3	HD 104237C	M/L	114H	–	–	–	–	55.6	−95.4	−30.8	–	–	–
4	HD 104237B	K/M	114H	–	–	–	–	55.6	−95.4	−30.8	–	–	–
5	HD 104237A	A7.75	114H	1.3	−11.6	−20.1	−10.9	55.6	−95.4	−30.8	7648	38.6	3.3/3.9
6	HD 104237D	M3.5	114H	–	–	–	–	55.6	−95.4	−30.8	3343	0.11	3.3/4.6
7	HD 104237E	K5.5	114H	–	–	–	–	55.6	−95.4	−30.8	4278	0.74	3.2/5.2
10	2MASS J12005517−7820296	M5.75	126	4.5	−12.8	−18.3	−6.4	61.2	−104.7	−34.2	3024	0.032	2.6/–
(29)	HD 104467	G3	102	2.1	−12.0	−18.8	−9.3	49.6	−84.4	−28.7	5830	4.0	8.1/12.3
11	2MASS J12014343−7835472	M2.25	100	5.7	−8.0	−24.7	−12.3	48.6	−82.9	−27.5	3524	0.0029	–
8	USNO-B 120144.7−781926	M5	100	1.5	−10.8	−21.4	−8.7	48.6	−83.1	−27.1	3125	0.027	7.5/8.9
9	CXOU J120152.8−781840	M4.75	121	3.0	−9.4	−21.4	−12.3	58.9	−100.5	−32.7	3161	0.042	5.3/7.1
(30)	RX J1202.1−7853	M0	110	2.9	−9.6	−23.1	−9.7	53.6	−91.0	−30.8	3850	0.43	2.2/3.0
(31)	RX J1204.6−7731	M3	112	4.0	−12.9	−17.6	−7.8	54.7	−93.4	−28.8	3415	0.22	1.4/2.5
(32)	RX J1207.7−7953	M3.5	111	1.2	−10.5	−20.6	−11.0	54.5	−91.0	−32.8	3343	0.11	3.2/4.5
(33)	HD 105923	G8	112	0.7	−10.7	−21.0	−9.6	54.9	−96.2	−16.7	5520	3.3	5.6/10.5
(34)	RX J1216.8−7753	M4	118	0.6	−10.8	−20.1	−10.5	58.8	−97.6	−30.8	3270	0.17	1.2/2.9
(35)	RX J1219.7−7403	M0	112	0.6	−11.0	−20.7	−9.4	56.1	−94.4	−22.0	3850	0.28	5.5/5.9
(36)	RX J1220.4−7407	M0	110	2.2	−11.9	−19.8	−8.1	55.2	−92.7	−21.7	3850	0.36	3.3/4.0
(37)	2MASS J12210499−7116493	K7	110	2.0	−11.8	−18.7	−10.2	55.2	−93.7	−16.4	4060	0.53	3.0/4.5
(38)	RX J1239.4−7502	K3	100	1.2	−10.7	−21.2	−9.0	52.0	−82.8	−21.1	4730	0.96	6.5/–
(39)	CD−69 1055	K0	99	0.6	−10.7	−21.0	−9.8	54.2	−81.8	−13.1	5250	1.5	9.2/15.6
(40)	MP Mus	K1	101	0.2	−10.7	−20.6	−9.9	58.4	−81.5	−12.2	5080	1.3	8.5/14.1

[a] ϵ Cha identification number (SIMBAD: [FLG2003] EPS CHA #). Values in parentheses are new members confirmed in this study, ordered by increasing RA.
[b] Suffix 'H' denotes a trigonometric distance from *Hipparcos*. All other distances are kinematic.
[c] Difference between the star and mean ϵ Cha space motion, see Section 5.2.
[d] Ages estimated from the Dotter et al. (2008) and Siess et al. (2000) models, respectively.

Table 8. Provisional members of the ϵ Cha association requiring confirmation.

ID	Name	Spectral type	Distance[b] (pc)	K^c	U	V	W	X	Y	Z	$T_{\rm eff}$	$L_{\rm bol}$	Age[d]
					(km s^{-1})				(pc)		(K)	($L_\odot$)	(Myr)
	TYC 9414-191-1	K5	105	–	–	–	–	47.4	−88.9	−29.7	4350	1.2	1.6/3.1
1	CXOU J115908.2−781232	M4.75	165	5.2	−10.2	−22.4	−5.1	79.9	−137.4	−44.4	3161	0.055	3.7/5.8
	RX J1202.8−7718[a]	M3.5	128	3.0	−9.7	−23.1	−9.7	62.3	−107.0	−32.5	3343	0.14	2.2/–
	HD 105234	A9	103H	–	–	–	–	50.5	−85.1	−28.5	7390	9.4	10.0/–
	HIP 59243	A6	94H	–	–	–	–	46.2	−77.5	−26.0	8350	15.8	7.9/9.0
	CM Cha[a]	K7	133	5.2	−9.3	−23.9	−6.4	71.4	−107.6	−31.7	4060	0.49	3.6/5.1

[a] Selected as kinematic member (see Appendix A).
[b] Suffix 'H' denotes a trigonometric distance from *Hipparcos*. All other distances are kinematic.
[c] Difference between the star and mean ϵ Cha space motion, see Section 5.2.
[d] Ages estimated from the Dotter et al. (2008) and Siess et al. (2000) models, respectively.

results of that study compared to our new ϵ Cha disc fraction. Fitting exponential decay models ($f_{\rm disc} = {\rm e}^{-t/\tau_0}$, with $f_{\rm disc,t=0} = 1$) to these data, they estimated that disc lifetimes in sparse associations were longer ($\tau_0 = 4.3 \pm 0.3$ Myr) than in denser environments ($\tau_0 = 2.8 \pm 0.1$ Myr). The latter time-scale agrees with similar fits by Mamajek (2009) (2.5 Myr) and Fedele et al. (2010) (3 Myr). With a larger and more complete membership, the updated ϵ Cha disc fraction now agrees with the general (dense) relation within the uncertainties.

Re-fitting the sparse associations, we derive a shorter characteristic time-scale of $\tau_0 = 3.8 \pm 0.5$ Myr, but one which is still $\sim 2\sigma$ longer than in denser environments. The fit is very sensitive to

Table 9. Candidates from the literature rejected as ϵ Cha members.

ID	Name	Reason[b]	Membership
	HD 82879[a]/82859	Binary	? Young
	RX J1137.4−7648	ΔM_I, dist, Li	Old field
	HIP 55746[a]	–	AB Dor
15	2MASS J11334926−7618399	dist	Cha I
	VW Cha	ΔM_I, dist	Cha I
	RX J1243.1−7458	dist	Cha II
14	RX J1123.2−7924	ΔM_I, Li	Octans?
12	2MASS J12074597−7816064	ΔM_I	? Young
19	RX J1150.4−7704	ΔM_I	? Young
	TYC 9238-612-1	ΔM_I	?
	TYC 9420-676-1	ΔM_I	?

[a]Selected as kinematic member (see Appendix A).
[b]ΔM_I: Photometry >1 mag from isochrone, dist = bad kinematic distance, Li = incongruous Li I λ6708 equivalent width.

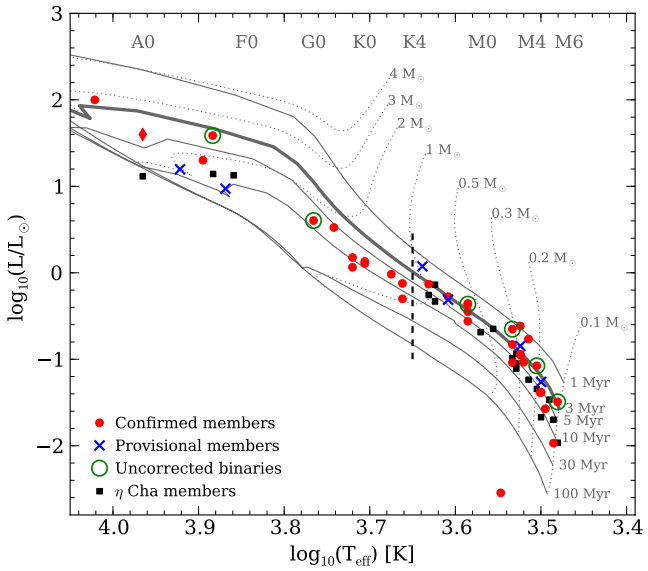

Figure 12. HR diagram of confirmed ϵ Cha members (red circles), provisional members (crosses) and η Cha members (squares). Uncorrected ϵ Cha binaries are circled. The filled diamond is ϵ Cha B (Feigelson et al. 2003). Pre-main-sequence mass tracks and isochrones from Dotter et al. (2008) are plotted for comparison. The dashed line at $\log_{10}T_{\rm eff} = 3.65$ is the limit of the low-mass sample (see the text).

the adopted disc fractions of η Cha and TW Hya. The former (28^{+10}_{-7} per cent) includes the seven dispersed halo members proposed by Murphy et al. (2010) but should be considered an upper limit as more halo members likely remain undiscovered. Additional members of TW Hya continue to be proposed (e.g. Schneider et al. 2012b, and references therein) and the membership of ϵ Cha is almost certainly incomplete, especially at lower masses. Although Fig. 18 provides some evidence for longer disc lifetimes in sparse associations (particularly in η Cha and TW Hya), given the incompleteness of these groups and the large uncertainties involved it may be pre-mature to draw firm conclusions until larger, more complete samples are available.

6.3.2 *Accretor frequency*

The strength of Hα emission is commonly used to identify stars actively accreting from circumstellar discs. The 32 members of

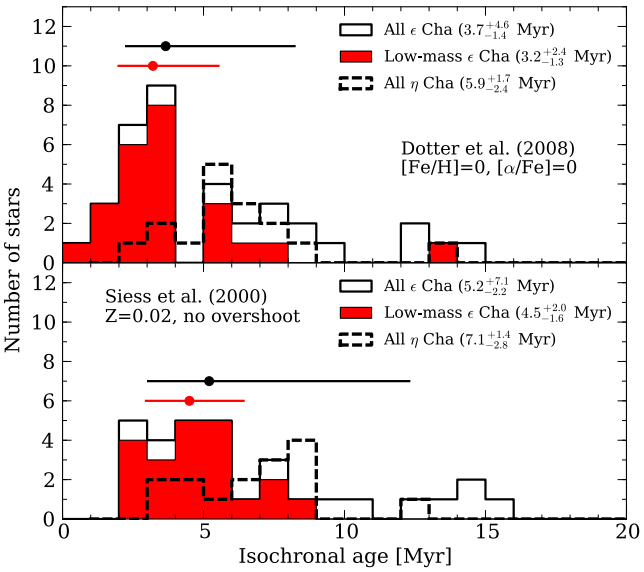

Figure 13. Ages derived from the Dotter et al. (2008) (top panel) and Siess et al. (2000) (bottom panel) isochrones. Stars with $\log_{10}T_{\rm eff} < 3.65$ are shown in red, the solid line is the envelope of all members. Dashed lines are η Cha members. Median ages are given in the legend and by the horizontal error bars (ϵ Cha only), with their 68 per cent confidence intervals.

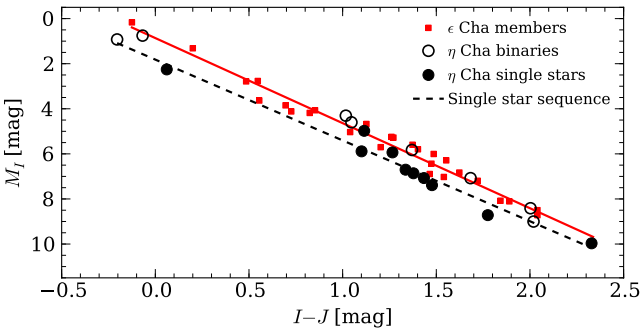

Figure 14. CMD with confirmed members of ϵ Cha (red squares) and the eight binary (Lyo et al. 2004a, open circles) and 10 single members of η Cha (filled circles). As predominantly equal-mass systems the binaries follow a sequence ∼0.75 mag above the single stars.

ϵ Cha with Hα EW measurements are plotted in Fig 19, excluding HD 104237D and E which were not resolved by *WISE*. EWs were measured from the WiFeS *R*7000 spectra by direct integration of the line profile. We estimate an uncertainty of 1 Å (rising to ∼3 Å for the broadest lines), primarily due to uncertainties defining the pseudo-continuum around the broad Hα lines at this modest spectral resolution. By the EW criteria of Fang et al. (2009) 10 stars (all with $K_s - {\rm W3} > 1.5$) are accreting.[8] HD 104237E is also accreting based on its disc excess (Fig. 16) and broad ($v_{10} \approx 500\,{\rm km\,s^{-1}}$) H$\alpha$ line (Feigelson et al. 2003). This is an accretor fraction of 32^{+9}_{-7} per cent (11/34). Fedele et al. (2010) proposed a similar exponential time-scale ($\tau_0 = 2.3$ Myr) for accretion in young groups. At ages of 3–5 Myr their relation predicts accretor fractions of ∼10–30 per cent, marginally consistent with our estimate.

[8] The EW of 2MASS J11404967−7459394 (ϵ Cha 16) flared to −35 Å on 2011 June 19 from its quiescent level around −11 Å. The star has no infrared excess and its Hα emission is likely chromospheric.

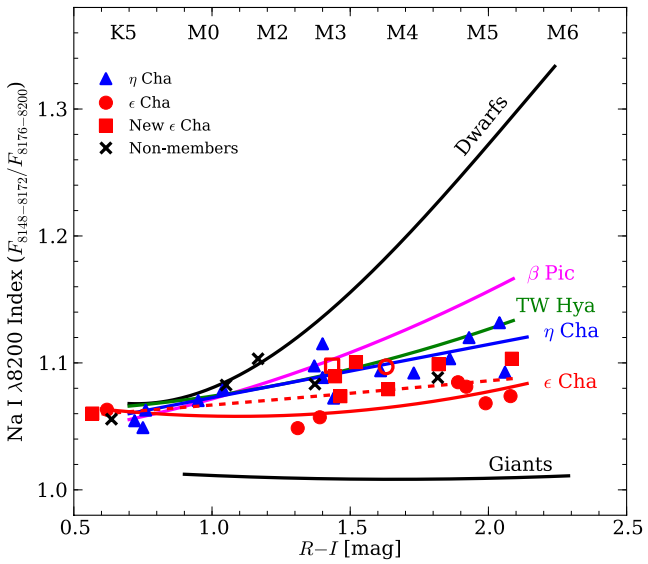

Figure 15. Na I λ8200 gravity indices of young associations. Solid lines are mean trends from Lawson, Lyo & Bessell (2009), with η and ϵ Cha members from Lyo et al. (2004b, 2008) (filled circles, triangles) and new ϵ Cha members observed with WiFeS (filled squares). Open symbols are the non-member 2MASS J12074597−7816064 (ϵ Cha 12) and provisional member RX J1202.8−7718. The dashed line is the new fit to all ϵ Cha members.

6.3.3 Notable T Tauri systems

The multi-epoch WiFeS observations revealed three accretors with broad, variable Hα emission. Velocity profiles of those stars are plotted in Fig. 20. They show asymmetric, multicomponent emission and velocity widths at 10 per cent of peak flux (v_{10}) in excess of the $v_{10} = 200$–270 km s^{-1} accretion threshold (Jayawardhana, Mohanty & Basri 2003). Note the large *daily* variation in the triple-peaked profiles of ϵ Cha 8. All three stars also exhibited He I λ5876/6678 emission and ϵ Cha 11 displayed strong forbidden [O I] λ6300/6363 and [N II] λ6584 emission. Using the v_{10} velocity widths and the relation of Natta et al. (2004), the accretion rates in these stars are $\sim 10^{-10}$–$10^{-8.5}$ M$_\odot$yr^{-1}, 1–2 orders of magnitude larger than those in η Cha (Lawson, Lyo & Muzerolle 2004; Murphy et al. 2011) and the TW Hya association (Muzerolle et al. 2000).

The spectrum of 2MASS J11183572−7935548 (ϵ Cha 13) is unique amongst ϵ Cha members, with strong Hα, Na I D, He I and forbidden [O I], [O II] λ7320/7331, [N II] λ6548/6583, [S II] λ6716/6731, [Ca II] λ7291/7324 and [Fe II] λ7155 emission lines all present (Fig. 21). While persistent over our 2010–11 observations, the emission is obviously variable as only the Hα line was present in the discovery spectrum of Luhman (2007). The star has a transitional disc with a large implied inner hole (Manoj et al. 2011), consistent with its narrower Hα line ($v_{10} \approx 170$ km s^{-1}) and smaller accretion rate (10^{-11} M$_\odot$ yr^{-1}). Forbidden emission typically arises in low-density, accretion-driven outflows or winds (Appenzeller & Mundt 1989). Such an outflow may have been responsible for clearing the inner region of ϵ Cha 13's disc.

6.4 Binaries in ϵ Cha

Six members of ϵ Cha are confirmed spectroscopic or visual binaries (RX J1158.5−7754A, RX J1220.4−7407, RX J1150.9−7411, RX J1204.6−7731, HD 104237A and ϵ Cha) and four stars are suspected of having a spectroscopic companion (ϵ Cha 10, 13, RX J1202.1−7853 and HD 104467). These give binary fractions of 21^{+10}_{-6} per cent (confirmed) and 36^{+10}_{-8} per cent (including suspected) when compared to the 18 single members with two or more radial velocity measurements. The core of η Cha has a similar binary fraction of 27–44 per cent (Lyo et al. 2004a), but lacks any systems with separations greater than 20 au (Brandeker et al. 2006).

6.4.1 Wide binaries

There are also several wide systems in ϵ Cha with projected separations of 10^3–10^4 au. We have already discussed HD 104237A–E (160–1700 au), RX J1158.5−7754AB (1700 au, hierarchical triple), T Cha AB (0.2 pc; Kastner et al. 2012) and the non-member HD 82879 (F4+F6, 2900 au). In addition to these systems, the M0 members RX J1219.7−7403 and RX J1220.4−7407 are separated by only 4.5 arcmin (0.14 pc at 110 pc) in the north of the association. The latter also has a 0.3 arcsec companion (Köhler 2001). Given their congruent radial velocities, proper motions and isolation they are highly likely to be physically associated. Several other wide pairs (HD 105234/HIP 59243, RX J1149.8−7850/RX J1147.7−7842 and HD 104467/RX J1202.1−7853) have incompatible kinematics or distances.

7 DISCUSSION

7.1 Relationship to η Chamaeleontis

The core of ϵ Cha is ∼10 deg (25 pc in space) from the young open cluster η Cha (Mamajek et al. 1999). Fig. 22 shows the distribution of their members on the sky. The groups share similar ages, distances and kinematics, which led Torres et al. (2008) to subsume the four members of η Cha with measured radial velocities at the time into their ϵ Cha solution. We did not consider these stars ϵ Cha members in this study. From the analysis of Section 6.2, it is now clear that the two groups are distinct, with subtly different properties.

Using the best-available space motions and positions from Mamajek et al. (2000), Jilinski, Ortega & de la Reza (2005) showed that the centres of η and ϵ Cha reached a minimum separation of ∼3 pc some 6–7 Myr ago. They concluded that the groups were born together or very close to one another in the outskirts of Sco–Cen. However, that study did not account for the large errors in the groups' space motions. Following the prescription of Makarov, Olling & Teuben (2004), our epicyclic traceback analysis (Fig. 23, top panel) replicates the Jilinski et al. result (red line), but shows that such a small separation is unlikely at any epoch given the quoted velocity uncertainties. Around 6–7 Myr ago fewer than 2 per cent of realizations resulted in a separation closer than 3 pc. With improved kinematics and positions for both groups (Table 6), it is clear that η and ϵ Cha were unlikely to have been much closer than their current separation and were ∼30 pc apart at the time of their birth (Fig. 23, bottom panel). This is further evidence that the two groups are distinct entities.

Any model for the birth of η and ϵ Cha must also account for their different physical characteristics. For example, to explain η Cha's apparently primordial deficit of wide (>20 au) binaries (Brandeker et al. 2006) and low-mass objects, Becker et al. (2013) speculated that the cluster was born in a small, highly magnetized cloud which prevented fragmentation on large scales. ϵ Cha was likely born under more quiescent conditions in a less-dense environment, as suggested by its larger spatial extent, the still-bound HD 104237A–E and a number of wider (10^3–10^4 au) systems. Moreover, the older

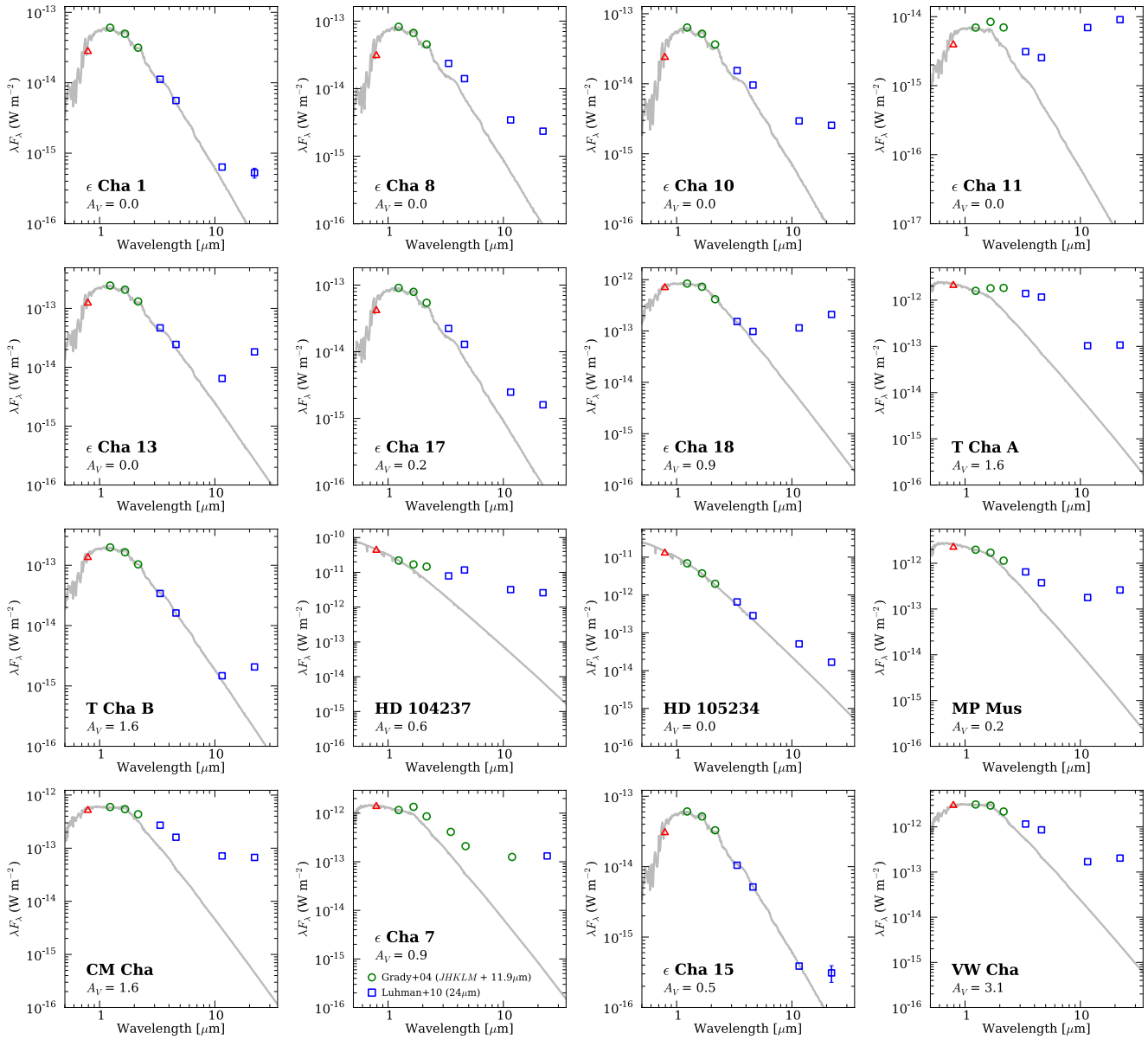

Figure 16. De-reddened DENIS (*i*, red triangle), 2MASS (*JHK*$_s$, green circles) and *WISE* (*W*1–*W*4, blue squares) 0.8–22 μm spectral energy distributions of ϵ Cha members with an infrared excess. Isophotal wavelengths and zero magnitude fluxes were taken from Fouqué et al. (2000), Cohen, Wheaton & Megeath (2003) and Jarrett et al. (2011). Flux errors are within the plotted points unless shown. The photospheric flux (grey line) is approximated by a solar metallicity, $\log g = 4.5$ MARCS model (Gustafsson et al. 2008) with similar effective temperature scaled to the *J*-band magnitude of each star. Photometry for ϵ Cha 7 (HD 104237E) comes from Grady et al. (2004) and Luhman et al. (2010). ϵ Cha 15 and VW Cha are kinematic members of Cha I.

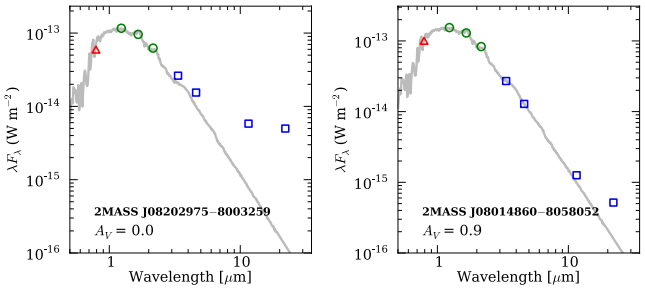

Figure 17. Same as Fig. 16, for the η Cha halo members 2MASS J08202975−8003259 and 2MASS J08014860−8058052. After reconsidering its photometry and optical spectrum, 2M J0801−80 has a spectral type of M4 and $A_V \approx 0.9$ (cf. Murphy et al. 2010).

wide binaries HD 82879/82859 and RX J0942.7−7726AB (Murphy et al. 2012) as well as several young stars whose origins are as-yet undetermined (e.g. Table 9) are hints that the star formation history of the region was more complex than the formation of two small groups in isolation a few Myr apart.

7.2 Star formation across the greater Sco–Cen region

Immediately north of ϵ Cha lies the LCC subgroup of the Sco–Cen (Fig. 22). LCC shows signs of spatio-kinematic substructure (Preibisch & Mamajek 2008) whereby the north of the subgroup appears older, richer and more distant (∼20 Myr, 120 pc) than the south (∼10 Myr, 110 pc). Recent work has also found an N-S gradient in the *W* velocity component (Mamajek, private communication).

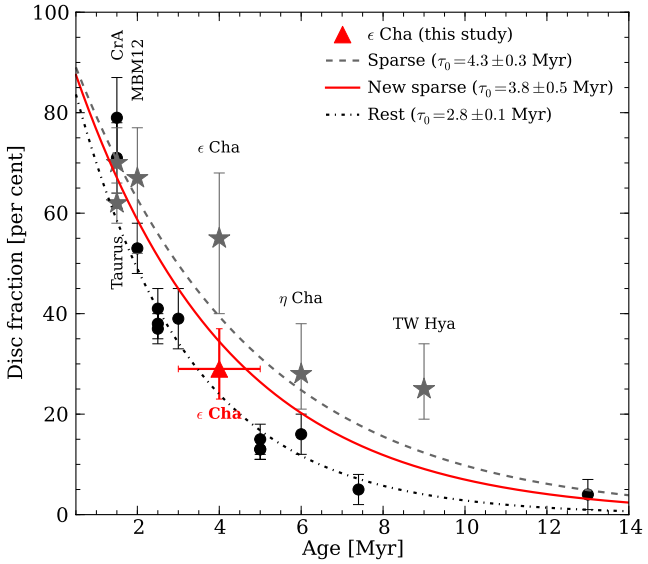

Figure 18. Disc frequencies for several clusters and star-forming regions from Fang et al. (2013). Sparse associations (TW Hya, η Cha, ϵ Cha, MBM12, Cr A, Taurus) are shown as filled stars. Lines show the exponential decay ($f_{\rm disc} = {\rm e}^{-t/\tau_0}$) models fitted to each environment. Our updated measurement for ϵ Cha (29^{+8}_{-6} per cent) is given by the red triangle.

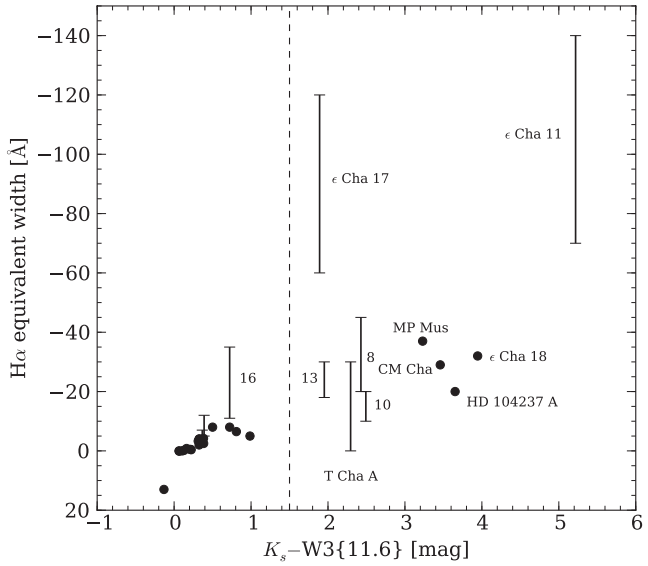

Figure 19. EW (negative values denote emission) of the Hα line versus the 2MASS/*WISE* $K_s - W3$ colour. With the exception of T Cha, all of the multi-epoch measurements (solid bars) are from our WiFeS *R*7000 observations. We classify as accretors those stars with $K_s - W3 > 1.5$ (dashed line), as well as HD 104237E (ϵ Cha 7).

These trends may be evidence for a wave of star formation starting in the north 15–20 Myr ago, spreading across the Galactic plane to form the southern part of the subgroup as well as the β Pic and TW Hya associations ∼10 Myr ago (Mamajek & Feigelson 2001) and ending with the birth of η and ϵ Cha as recently as 3–5 Myr ago.

2MASS J12210499−7116493 (Kiss et al. 2011) and four stars proposed by Torres et al. (2008) lie north of the majority of ϵ Cha members within the southern reaches of LCC. Mamajek et al. (2002) attributed the four stars to LCC in their survey of solar-type Sco–Cen members and they also have isochronal ages in Table 7 older than the majority of ϵ Cha members (although there may be

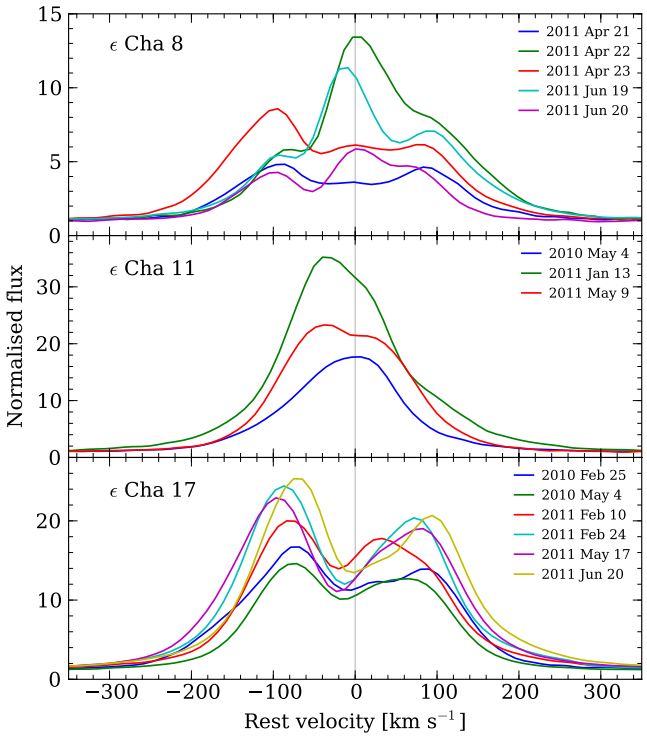

Figure 20. WiFeS/*R*7000 velocity profiles for ϵ Cha members with complex Hα emission lines; USNO-B 120144.7−781926 (ϵ Cha 8), 2MASS J12014343−7835472 (ϵ Cha 11) and 2MASS J11432669−7804454 (ϵ Cha 17). All of the profiles are shifted to zero radial velocity.

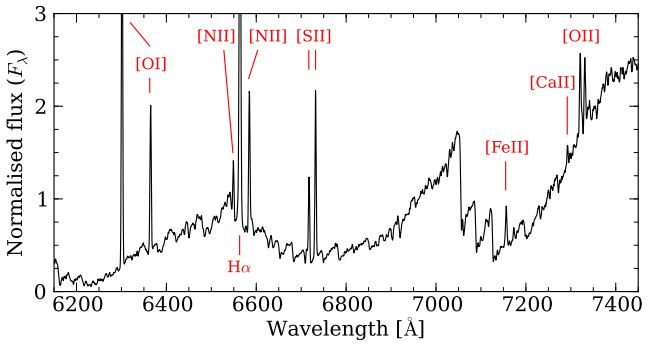

Figure 21. WiFeS/*R*3000 spectrum of 2MASS J11183572−7935548 (ϵ Cha 13). The star exhibits strong Hα and the forbidden line emission typical of a Classical T Tauri star.

systematic errors in the ages of solar-type stars, see Section 6.2). Table 10 compares their observed and expected kinematics. With the exception of CP−68 1388, which is a marginally better match to LCC ($\Delta K = 1$ km s^{-1}), their proper motions and radial velocities agree with the space motion of ϵ Cha at 100–110 pc. The 80–90 pc distances implied by membership in LCC are well below the 100–120 pc typically attributed to the subgroup. Furthermore, the K7 2MASS J12210499−7116493 has an Li I λ6708 EW much greater than similar LCC members recently proposed by Song et al. (2012) (or the roughly coeval β Pic). At the late-G and early-K spectral types of the four Torres et al. members there is little difference in lithium depletion at ages $\lesssim$20 Myr. Pending better knowledge of the low-mass population of southern LCC, we retain these stars as members of ϵ Cha as defined in this study (but see below).

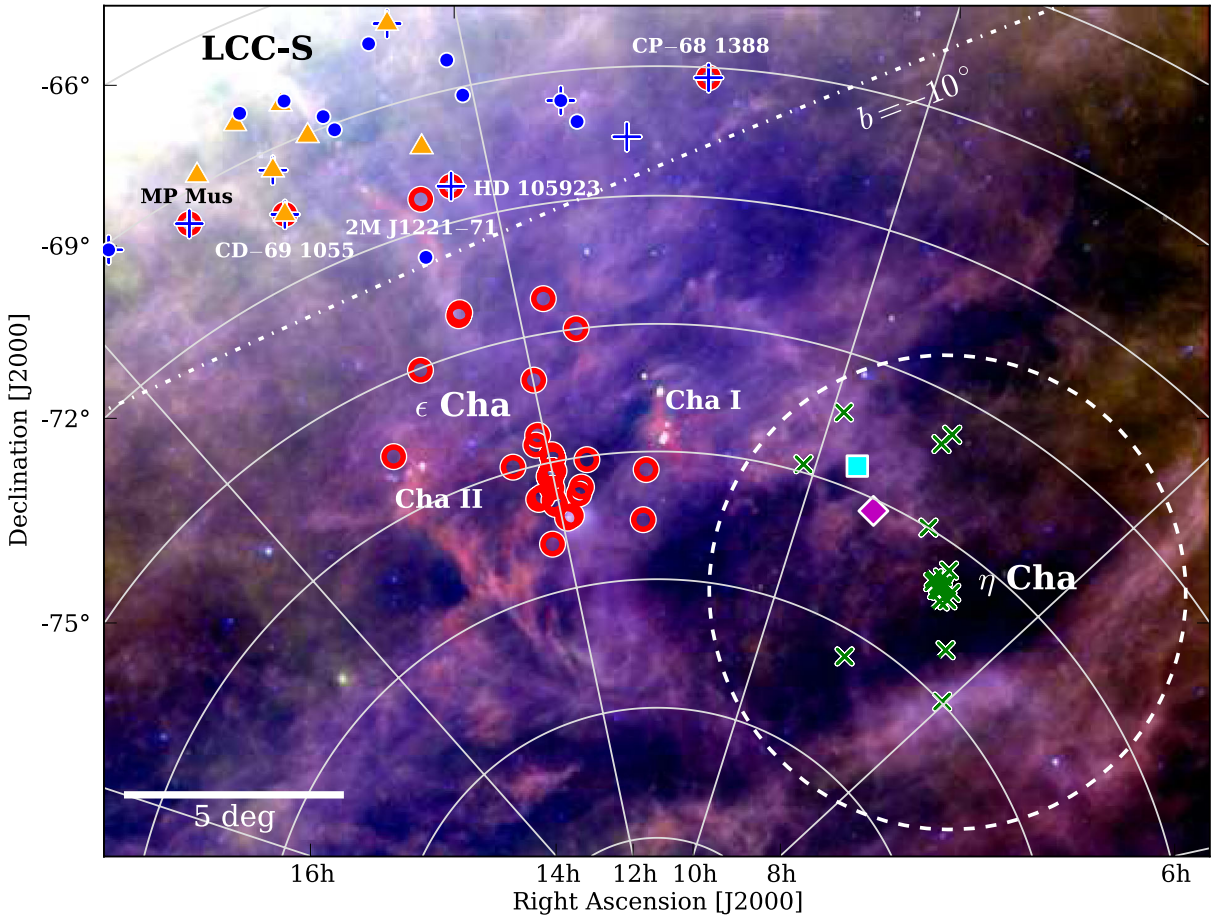

Figure 22. *IRAS* 100/60/25 μm colour composite with η Cha members (green crosses) and confirmed or provisional members of ϵ Cha (open circles). Stars discussed in the text are labelled. The diamond and square are the wide systems HD 82879/82859 and RX J0942.7–7726AB, respectively. LCC members from Preibisch & Mamajek (2008) (blue pluses), de Zeeuw et al. (1999) (filled circles) and Song, Zuckerman & Bessell (2012) (triangles) are shown with the $b = -10°$ 'boundary' of the subgroup (dot dashed line). The dashed line is the 5.5 deg radius around η Cha surveyed for new members by Murphy et al. (2010).

However, given their similar ages, kinematics, distances and the observed trends in these parameters, a useful demarcation between the southern extent of LCC and ϵ Cha may simply not exist. In this scenario, it is possible that the four Torres et al. (2008) stars in Table 10 could be comoving with ϵ Cha and have similar ages but were not born near the majority of its members. Song et al. (2012) have identified several young, low-mass stars immediately north of ϵ Cha (Fig. 22) and the provisional candidate RX J1202.8−7718 may be an outlying LCC member juxtaposed on the central region of ϵ Cha. A similar problem exists at the northern boundary of LCC and TW Hya, where young stars at 70–150 pc have ambiguous memberships (Lawson & Crause 2005; Mamajek 2005). Clarifying this messy picture of star formation will require a larger sample of young stars with reliable distances and ages. The soon-to-be-launched *Gaia* mission will help immensely in this regard.

In the interim, we can only speculate how η and ϵ Cha formed within the greater Sco–Cen region. A schematic picture was provided by Feigelson (1996), who proposed young stars born in different parts of a dynamically unbound giant molecular cloud (GMC) are dispersed by internal turbulent velocities. In this picture, some parts of the GMC may collapse quickly to form rich clusters while other regions remain stable against collapse as they disperse, forming stellar aggregates of a range of ages and sizes over wide areas. Preibisch & Mamajek (2008) proposed that the bulk of star formation in Sco–Cen probably proceeded in this way as a series of small clusters and filaments, each containing tens to hundreds of stars. The local virial balance of the nascent cloudlets meant some resulting groups are compact (η Cha and the core of ϵ Cha), while others appear unbound and widely dispersed (e.g. TW Hya, β Pic and the outer members of ϵ Cha) (Feigelson et al. 2003).

8 SUMMARY

We have critically re-examined membership of the young ϵ Cha association using the best available spectroscopic and kinematic information. The main results of this study are as follows.

(1) Of the 52 candidates proposed in the literature, we confirm 35 stars as members, with spectral types of B9 to mid-M. Six candidates are classified as provisional members requiring better kinematics, trigonometric parallaxes or binary information.

(2) ϵ Cha lies at a mean distance of 110 ± 7 pc and has a mean space motion of $(U, V, W) = (-10.9 \pm 0.8, -20.4 \pm 1.3, -9.9 \pm 1.4)$ km s^{-1}. Comparison of its HRD to theoretical evolutionary models yields a median age of 3–5 Myr, distinguishing it as the youngest moving group in the solar neighbourhood.

(3) 15 members have infrared SEDs attributable to circumstellar discs, including 11 stars whose strong Hα emission indicates they are accreting. As expected of a rapidly evolving intermediate-age population, these stars show a variety of SED morphologies, from

Table 10. Observed and predicted kinematics of northern ϵ Cha/LCC members.

MML ID[a]	Star	Observed ($\mu_\alpha \cos\delta$, μ_δ)† (mas yr^{-1})		RV‡ (km s^{-1})	ϵ Cha ($\mu_\alpha \cos\delta$, μ_δ) (mas yr^{-1})		RV (km s^{-1})	$d_{\rm kin}$ (pc)	LCC (Chen et al. 2011) ($\mu_\alpha \cos\delta$, μ_δ) (mas yr^{-1})		RV (km s^{-1})	$d_{\rm kin}$ (pc)
	2M J1221−71	−39.4	−11.8	11.5	−39	−11	13.4	110	−42	−4	14.6	89
1	CP−68 1388	−36.1	+5.7	15.9	−37	+2	15.8	112	−36	+8	16.7	91
7	HD 105923	−38.9	−8.3	14.2	−39	−9	13.7	112	−40	−3	14.9	92
27	CD−69 1055	−43.1	−18.7	12.8	−43	−19	12.2	99	−46	−12	13.6	82
34	MP Mus	−40.8	−23.0	11.6	−41	−23	11.4	101	−45	−17	12.9	84

[a]Identifier from Mamajek et al. (2002).
[b]Proper motions from Tycho-2 and SPM4 (2MASS J12210499−7116493).
[c]Radial velocities from Torres et al. (2006) and Kiss et al. (2011) (2MASS J12210499−7116493).

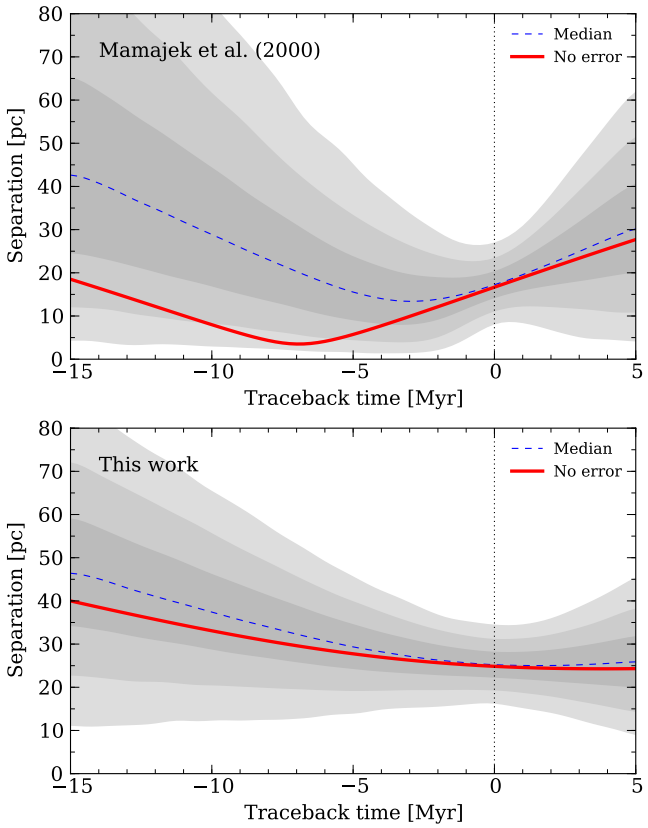

Figure 23. Separation between η Cha and the core of ϵ Cha as a function of time. Top: initial positions and velocities from Mamajek et al. (2000). Bottom: updated values from Table 6. The solid line assumes no errors on the position or velocity of either association while the shaded regions are the 16–84, 2–98 and 0.1–99.9 per cent contours of the cumulative distribution ($\pm$1–3σ) from 5000 realizations. In both panels, the initial centre of ϵ Cha is assumed normally distributed in *XYZ* with $\sigma = 3$ pc.

optically thick accretion discs, to weak-excess debris discs. Both the disc and accretion fractions (29^{+8}_{-6} and 32^{+9}_{-7} per cent, respectively) are consistent with a typical 3–5 Myr old population.

(4) A comparative age analysis shows that ϵ Cha is approximately 1–3 Myr younger than the nearby open cluster η Cha. Contrary to previous studies which assumed η and ϵ Cha are coeval and formed in the same location, we find the groups were separated by ∼30 pc when η Cha was born, followed soon after by ϵ Cha.

(5) The physical properties, locations and kinematics of η and ϵ Cha are consistent with them being formed in the turbulent interstellar medium surrounding the Sco–Cen. They are likely the products of the last burst of star formation in southern Sco–Cen, which earlier formed the sparse TW Hya and β Pic groups and several thousand older (now field) stars.

(6) After considering all the available observations, we rejected several proposed members. They instead belong to the background Cha I and II cloud populations and other nearby young groups. In the absence of parallaxes and precise stellar ages, we emphasize the importance of a holistic and conservative approach to assigning stars to kinematic groups, many of which have only subtly different properties and ill-defined memberships.

(7) In this study, we considered only those stars proposed as members in the literature. There are likely many new members of ϵ Cha awaiting discovery in contemporary proper motions catalogues (e.g. SPM4, PPMXL). These candidates can be tested against the definition of ϵ Cha presented here to extend its membership to lower masses and wider areas.

ACKNOWLEDGEMENTS

We thank Pavel Kroupa, Eric Mamajek and Eric Feigelson for their considered comments on the thesis of SJM from which this work is based, and the anonymous referee for their thorough review of the manuscript. We also thank the ANU TAC for their generous allocation of telescope time. This research has made extensive use of the VizieR and SIMBAD services provided by CDS, Strasbourg and the TOPCAT software package developed by Mark Taylor (U. Bristol). Many catalogues used in this work are hosted by the German Astrophysical Virtual Observatory. *WISE* is a joint project of the University of California, Los Angeles and the Jet Propulsion Laboratory/California Institute of Technology, funded by NASA. 2MASS is a joint project of the University of Massachusetts and the Infrared Processing and Analysis Centre/California Institute of Technology, funded by NASA and the NSF.

REFERENCES

Alcala J. M., Krautter J., Schmitt J. H. M. M., Covino E., Wichmann R., Mundt R., 1995, A&AS, 114, 109
Appenzeller I., Mundt R., 1989, A&AR, 1, 291
Baraffe I., Chabrier G., 2010, A&A, 521, A44
Barbier-Brossat M., Figon P., 2000, A&AS, 142, 217
Barrado y Navascues D., 1998, A&A, 339, 831
Becker C., Moraux E., Duchêne G., Maschberger T., Lawson W., 2013, A&A, 552, A46
Böhm T., Catala C., Balona L., Carter B., 2004, A&A, 427, 907
Brandeker A., Liseau R., Artymowicz P., Jayawardhana R., 2001, ApJ, 561, L199
Brandeker A., Jayawardhana R., Khavari P., Haisch K. E., Jr, Mardones D., 2006, ApJ, 652, 1572

Cameron E., 2011, PASA, 28, 128
Carpenter J. M., 2001, AJ, 121, 2851
Chen C. H., Mamajek E. E., Bitner M. A., Pecaut M., Su K. Y. L., Weinberger A. J., 2011, ApJ, 738, 122
Cohen M., Wheaton W. A., Megeath S. T., 2003, AJ, 126, 1090
Correia S., Zinnecker H., Ratzka T., Sterzik M. F., 2006, A&A, 459, 909
Covino E., Alcala J. M., Allain S., Bouvier J., Terranegra L., Krautter J., 1997, A&A, 328, 187
Currie T., Thalmann C., Matsumura S., Madhusudhan N., Burrows A., Kuchner M., 2011, ApJ, 736, L33
Cutispoto G., Pastori L., Pasquini L., de Medeiros J. R., Tagliaferri G., Andersen J., 2002, A&A, 384, 491
da Silva L., Torres C. A. O., de La Reza R., Quast G. R., Melo C. H. F., Sterzik M. F., 2009, A&A, 508, 833
de Zeeuw P. T., Hoogerwerf R., de Bruijne J. H. J., Brown A. G. A., Blaauw A., 1999, AJ, 117, 354
Dopita M., Hart J., McGregor P., Oates P., Bloxham G., Jones D., 2007, Ap&SS, 310, 255
Dotter A., Chaboyer B., Jevremović D., Kostov V., Baron E., Ferguson J. W., 2008, ApJS, 178, 89
Ducourant C., Teixeira R., Périé J. P., Lecampion J. F., Guibert J., Sartori M. J., 2005, A&A, 438, 769
Epchtein N. et al., 1999, A&A, 349, 236
Fang M., van Boekel R., Wang W., Carmona A., Sicilia-Aguilar A., Henning T., 2009, A&A, 504, 461
Fang M., van Boekel R., Bouwman J., Henning T., Lawson W. A., Sicilia-Aguilar A., 2013, A&A, 549, A15
Fedele D., van den Ancker M. E., Henning T., Jayawardhana R., Oliveira J. M., 2010, A&A, 510, A72
Feigelson E. D., 1996, ApJ, 468, 306
Feigelson E. D., Lawson W. A., Garmire G. P., 2003, ApJ, 599, 1207
Fouqué P. et al., 2000, A&AS, 141, 313
Franchini M., Covino E., Stalio R., Terranegra L., Chavarria -K. C., 1992, A&A, 256, 525
Frink S., Roeser S., Alcala J. M., Covino E., Brandner W., 1998, A&A, 338, 442
Girard T. M. et al., 2011, AJ, 142, 15
Grady C. A. et al., 2004, ApJ, 608, 809
Grenier S., Burnage R., Faraggiana R., Gerbaldi M., Delmas F., Gómez A. E., Sabas V., Sharif L., 1999, A&AS, 135, 503
Guenther E. W., Esposito M., Mundt R., Covino E., Alcalá J. M., Cusano F., Stecklum B., 2007, A&A, 467, 1147
Gustafsson B., Edvardsson B., Eriksson K., Jørgensen U. G., Nordlund Å., Plez B., 2008, A&A, 486, 951
Haisch K. E., Jr, Lada E. A., Lada C. J., 2001, ApJ, 553, L153
Høg E. et al., 2000, A&A, 355, L27
James D. J., Melo C., Santos N. C., Bouvier J., 2006, A&A, 446, 971
Jarrett T. H. et al., 2011, ApJ, 735, 112
Jayawardhana R., Mohanty S., Basri G., 2003, ApJ, 592, 282
Jilinski E., Ortega V. G., de la Reza R., 2005, ApJ, 619, 945
Kastner J. H., Thompson E. A., Montez R., Murphy S. J., Bessell M. S., Sacco G., 2012, ApJ, 747, L23
Kenyon S. J., Hartmann L., 1995, ApJS, 101, 117
Kiss L. L. et al., 2011, MNRAS, 411, 117
Knude J., 2010, preprint (astro-ph/1006.3676)
Knude J., Hog E., 1998, A&A, 338, 897
Köhler R., 2001, AJ, 122, 3325
Kraus A. L., Hillenbrand L. A., 2007, AJ, 134, 2340
Lawson W. A., Crause L. A., 2005, MNRAS, 357, 1399
Lawson W. A., Crause L. A., Mamajek E. E., Feigelson E. D., 2001, MNRAS, 321, 57
Lawson W. A., Lyo A. R., Muzerolle J., 2004, MNRAS, 351, L39
Lawson W. A., Lyo A., Bessell M. S., 2009, MNRAS, 400, L29
Lopez Martí B., Jimenez Esteban F., Bayo A., Barrado D., Solano E., Rodrigo C., 2013, A&A, 551, A46
Luhman K. L., 2004a, ApJ, 602, 816
Luhman K. L., 2004b, ApJ, 616, 1033
Luhman K. L., 2007, ApJS, 173, 104
Luhman K. L., 2008, in Reipurth B., ed., Handbook of Star Forming Regions, Vol. II: The Southern Sky. Astron. Soc. Pac., San Francisco, p. 169
Luhman K. L., Steeghs D., 2004, ApJ, 609, 917
Luhman K. L., Stauffer J. R., Muench A. A., Rieke G. H., Lada E. A., Bouvier J., Lada C. J., 2003, ApJ, 593, 1093
Luhman K. L. et al., 2008, ApJ, 675, 1375
Luhman K. L., Allen P. R., Espaillat C., Hartmann L., Calvet N., 2010, ApJS, 186, 111
Lyo A. R., Lawson W. A., Feigelson E. D., Crause L. A., 2004a, MNRAS, 347, 246
Lyo A. R., Lawson W. A., Bessell M. S., 2004b, MNRAS, 355, 363
Lyo A. R., Lawson W. A., Bessell M. S., 2008, MNRAS, 389, 1461
Makarov V. V., Olling R. P., Teuben P. J., 2004, MNRAS, 352, 1199
Malo L., Doyon R., Lafrenière D., Artigau É., Gagné J., Baron F., Riedel A., 2013, ApJ, 762, 88
Mamajek E. E., 2005, ApJ, 634, 1385
Mamajek E. E., 2009, in Usuda T., Tamura M., Ishii M., eds, Proc. AIP Conf. Ser., Vol. 1158, Exoplanets and Disks: Their Formation and Diversity. Am. Inst. Phys., New York, p. 3
Mamajek E. E., Feigelson E. D., 2001, in Jayawardhana R., Greene T., eds, ASP Conf. Ser. Vol. 244, Young Stars Near Earth: Progress and Prospects. Astron. Soc. Pac., San Francisco, p. 104
Mamajek E. E., Lawson W. A., Feigelson E. D., 1999, ApJ, 516, L77
Mamajek E. E., Lawson W. A., Feigelson E. D., 2000, ApJ, 544, 356
Mamajek E. E., Meyer M. R., Liebert J., 2002, AJ, 124, 1670
Manoj P. et al., 2011, ApJS, 193, 11
Mentuch E., Brandeker A., van Kerkwijk M. H., Jayawardhana R., Hauschildt P. H., 2008, ApJ, 689, 1127
Murphy S. J., Lawson W. A., Bessell M. S., 2010, MNRAS, 406, L50
Murphy S. J., Lawson W. A., Bessell M. S., Bayliss D. D. R., 2011, MNRAS, 411, L51
Murphy S. J., Lawson W. A., Bessell M. S., 2012, MNRAS, 424, 625
Muzerolle J., Calvet N., Briceño C., Hartmann L., Hillenbrand L., 2000, ApJ, 535, L47
Nakajima T., Morino J. I., 2012, AJ, 143, 2
Natta A., Testi L., Muzerolle J., Randich S., Comerón F., Persi P., 2004, A&A, 424, 603
Nehmé C., Gry C., Boulanger F., Le Bourlot J., Pineau Des Forêts G., Falgarone E., 2008, A&A, 483, 471
Nordström B. et al., 2004, A&A, 418, 989
Perryman M. A. C. et al., 1997, A&A, 323, L49
Pickles A. J., 1998, PASP, 110, 863
Preibisch T., Mamajek E. E., 2008, in Reipurth B., ed., Handbook of Star Forming Regions, Vol. II, The Southern Sky. Astron. Soc. Pac., San Francisco, p. 235
Riaz B., Gizis J. E., Harvin J., 2006, AJ, 132, 866
Riddick F. C., Roche P. F., Lucas P. W., 2007, MNRAS, 381, 1067
Röser S., Demleitner M., Schilbach E., 2010, AJ, 139, 2440
Schisano E., Covino E., Alcalá J. M., Esposito M., Gandolfi D., Guenther E. W., 2009, A&A, 501, 1013
Schlegel D. J., Finkbeiner D. P., Davis M., 1998, ApJ, 500, 525
Schneider A., Melis C., Song I., 2012a, ApJ, 754, 39
Schneider A., Song I., Melis C., Zuckerman B., Bessell M., 2012b, ApJ, 757, 163
Shkolnik E., Liu M. C., Reid I. N., 2009, ApJ, 699, 649
Sicilia-Aguilar A. et al., 2009, ApJ, 701, 1188
Siess L., Dufour E., Forestini M., 2000, A&A, 358, 593
Simon M., Schlieder J. E., Constantin A. M., Silverstein M., 2012, ApJ, 751, 114
Skrutskie M. F. et al., 2006, AJ, 131, 1163
Soderblom D. R., Jones B. F., Balachandran S., Stauffer J. R., Duncan D. K., Fedele S. B., Hudon J. D., 1993, AJ, 106, 1059
Song I., Bessell M. S., Zuckerman B., 2002, ApJ, 581, L43
Song I., Zuckerman B., Bessell M. S., 2012, AJ, 144, 8
Spezzi L. et al., 2008, ApJ, 680, 1295
Terranegra L., Morale F., Spagna A., Massone G., Lattanzi M. G., 1999, A&A, 341, L79

Torres C. A. O., Quast G. R., da Silva L., de La Reza R., Melo C. H. F., Sterzik M., 2006, A&A, 460, 695
Torres C. A. O., Quast G. R., Melo C. H. F., Sterzik M. F., 2008, in Reipurth B., ed., Handbook of Star Forming Regions, Vol. II: The Southern Sky. Astron. Soc. Pac., San Francisco, p. 757
van Leeuwen F., 2007, A&A, 474, 653
Wahhaj Z. et al., 2010, ApJ, 724, 835
Wichmann R., Schmitt J. H. M. M., Hubrig S., 2003, A&A, 399, 983
Williams J. P., Cieza L. A., 2011, ARA&A, 49, 67
Wright E. L. et al., 2010, AJ, 140, 1868
Zacharias N., Finch C. T., Girard T. M., Henden A., Bartlett J. L., Monet D. G., Zacharias M. I., 2013, AJ, 145, 44
Zboril M., Byrne P. B., Rolleston W. R. J. R., 1997, MNRAS, 284, 685
Zuckerman B., Song I., 2004, ARA&A, 42, 685

APPENDIX A: NOTES ON INDIVIDUAL CANDIDATES

A1 Confirmed members

CXOU J120152.8−781840 (ϵ Cha 9) – Fang et al. (2013) questioned membership of this star based on its PPMXL proper motion. It was not recovered in UCAC4 but using higher precision SPM4 astrometry we find that it is a kinematic member at 121 pc.

RX J1149.8−7850 (ϵ Cha 18) – Malo et al. (2013) assigned the star to β Pic. Their Bayesian analysis (which did not include ϵ Cha) gave a distance of 71 pc, which would make it one of the most distant members. Given its large Li I λ6708 EW it is likely younger than β Pic and we find an excellent match to ϵ Cha at a distance of 110 pc.

RX J1150.9−7411 – using the Terranegra et al. (1999) proper motion (Section 4.1.2), we find RX J1150.9−7411 to be a kinematic member at 108 pc. The star has a close companion (Köhler 2001) and we caution that the WiFeS velocity may not be systemic.

RX J1158.5−7754AB (ϵ Cha 21+20) – the 104 pc kinematic distance adopted for RX J1158.5−7754A just agrees with its *Hipparcos* parallax (90.4^{+14}_{-11} pc). Köhler (2001) detected a 0.07 arcsec companion and the system is only 16 arcsec from ϵ Cha 20 (GSC 9415–2676, $d_{\rm kin} = 119$ pc). Perhaps as well as being responsible for the velocity variation (Table 5), the close companion distorted the parallax over the short-baseline *Hipparcos* observations. The triple system is only 5 arcmin from HD 104036, which has a *Hipparcos* distance of 108 ± 4 pc.

HD 104237A (ϵ Cha 5) – a core member of ϵ Cha, the Herbig Ae star has a space motion only 1.3 km s^{-1} from the mean and a kinematic distance which agrees with its 114 pc *Hipparcos* parallax. HD 104237A was rejected in the convergent analysis because of its position above the isochrone. This is likely due to a combination of binarity (Böhm et al. 2004), infrared excess and an uncertain spectral type/reddening (Lyo et al. 2008).

HD 104237B–E (ϵ Cha 3–7) – all four late-type components of the HD 104237 system show X-ray emission and are almost certainly associated with their primary. Fang et al. (2013) estimated the mass of HD 104237C to be 13–15 $M_{\rm Jup}$ from NIR photometry, making it the lowest mass member of ϵ Cha. Components *D* and *E* have strong lithium absorption. Both stars were rejected from the convergent solution by their discrepant kinematics. Their proper motions (and the photometry of HD 104237D) are likely influenced by HD 104237A.

2MASS J12014343−7835472 (ϵ Cha 11) – we find an excellent proper motion match at 100 pc with a predicted radial velocity 6 km s^{-1} lower than measured. This may be due to unresolved binarity or strong accretion activity (see Section 6.3.3). Three WiFeS velocities showed no trend over ∼1 yr. Luhman (2004b) attributed its underluminosity to obscuration by an edge-on circumstellar disc. This was confirmed by Fang et al. (2013). We confirm membership in ϵ Cha based on a congruent proper motion, Li I EW and location in the core of the association.

A2 Provisional members

CXOU J115908.2−781232 (ϵ Cha 1) – the smaller proper motion yields a kinematic distance of 165 pc ($K = 5.2$ km s^{-1}). The star is unlikely to have been ejected from the core as its predicted radial velocity is only ∼1 km s^{-1} from observed. ϵ Cha 1 is not found in UCAC4 but its PPMXL proper motion ($\mu_{\alpha\cos\delta}$, $\mu_\delta = -36 \pm 14$, -6 ± 14 mas yr^{-1}) is consistent with membership at 120 pc ($K = 1.5$ km s^{-1}), notwithstanding the large errors. Given its location near the centre of ϵ Cha, we assign it provisional membership pending better kinematics.

RX J1202.8−7718 – in the absence of accelerated lithium depletion (e.g. Baraffe & Chabrier 2010) the star's 300 mÅ Li I λ6708 EW suggests an age closer to the TW Hya and β Pic associations (8–12 Myr). The only nearby population with a similar age is the LCC subgroup of Sco–Cen, whose southern extent may be as young as ∼10 Myr (see Section 7.2). RX J1202.8−7718 is an equally good match to the LCC space motion (Chen et al. 2011) at 110 pc. Given its location close to the core of ϵ Cha we retain it as a provisional member, though it may be an older, dispersed member of Sco–Cen.

CM Cha – previously assigned to Cha II, the star was tentatively reclassified as a member of ϵ Cha by Lopez Martí et al. (2013) by its UCAC3 proper motion. With SPM4, we find a somewhat poor ($K = 5.2$ km s^{-1}) kinematic match to ϵ Cha at 133 pc. A marginally better match to Cha II (Lopez Martí et al. 2013) is found at ∼120 pc, though this is considerably closer than recent distance estimates to the cloud (180–210 pc; Knude 2010). Given its location near Cha II and discordant proper motions (see Section 4.1.2), we assign provisional membership in ϵ Cha and await improved kinematics or a parallax.

A3 Non-members

HD 82879 – The F6 star is only 24 arcsec from and comoving with HD 82859 (F4, Fig. A1). It is associated with the *ROSAT* X-ray

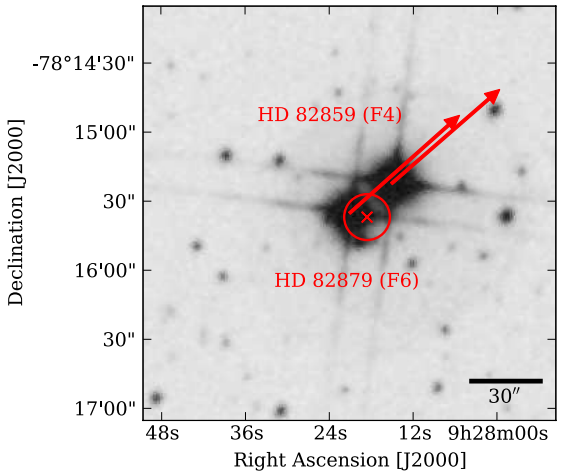

Figure A1. POSS2-Red 3×3 arcmin image centred on HD 82879. Arrows show the Tycho-2 proper motions over 2000 yr. The cross and circle give the position of the *ROSAT* source (RX J0928.5−7815) and its uncertainty.

source RX J0928.5−7815 and was proposed as an ϵ Cha member by Torres et al. (2008). Lopez Martí et al. (2013) also listed it as a member but neither study noted its binarity. HD 82879 is a good isochronal and kinematic match to ϵ Cha. However, given its large total mass ($\sim$2.8 $M_\odot$) and isolation it is unlikely the system could have been dispersed from ϵ or η Cha within their lifetimes. Neither star was observed by *Hipparcos* but HD 82859 has an ill-constrained Tycho-2 parallax of 110^{+330}_{-50} pc. da Silva et al. (2009) suggested HD 82879 as a member of the AB Doradus association; however, we find a poor kinematic match at any distance.

HIP 55746 – this star has the largest offset from the mean ϵ Cha space motion ($K = 6.7\,\mathrm{km\,s^{-1}}$) and is the closest proposed member (89 ± 5 pc, *Hipparcos*). However, it is only $3\,\mathrm{km\,s^{-1}}$ from the space motion of AB Dor (Torres et al. 2008) with a distance similar to other members. We follow Torres et al. (2008) and assign the star to AB Dor.

RX J1137.4−7648 – despite the excellent kinematic match ($K = 1.7\,\mathrm{km\,s^{-1}}$), the 4 mag underluminosity, outlying distance (67 pc) and lack of Li I λ6708 absorption rule RX J1137.4−7648 out as a member of ϵ Cha. The 3-arcsec visual binary is likely an nearby, older field system.

2MASS J11334926−7618399 (ϵ Cha 15) – located between Cha I and the core of ϵ Cha, the star was proposed by Luhman et al. (2008) as having a proper motion (not reported in that work) more similar to ϵ Cha than the cloud sources. Although it lies on the mean isochrone only $2.6\,\mathrm{km\,s^{-1}}$ from the ϵ Cha space motion, its 197 pc distance is much greater than other members. The star is not in the USNO-B1 or UCAC catalogues and its SuperCosmos proper motion is erroneous. Its PPMXL and SPM4 kinematics and modest reddening are consistent with an outlying Cha I member at a distance of $\sim$160 pc.

RX J1243.1−7458 – the close binary (Köhler 2001) lies a few degrees north of Cha II and its space motion gives a reasonable agreement ($K = 3.7\,\mathrm{km\,s^{-1}}$) with the cloud sources at $\sim$260 pc. This is considerably larger than recent distance estimates to the cloud (180–210 pc; Knude 2010). If we use the Terranegra et al. (1999) proper motion, a better match is found at 200 pc. The predicted radial velocity agrees with the mean WiFeS value, implying we observed the star close to its systemic velocity. We classify RX J1243.1−7458 as an outlying member of Cha II, but caution that its proper motion may be affected by the close companion.

VW Cha – the star is unlikely to be a member of ϵ Cha based on its large implied distance (217 pc) and position well above the isochrone. It was classified as a Cha I member by Luhman (2007) and again by Lopez Martí et al. (2013). Its proper motion, large extinction and location inside the southern cloud core support this assignment. We find the best match to the Cha I space motion at $\sim$160 pc, the distance to the cloud.

RX J1150.4−7704 (ϵ Cha 19) – Torres et al. (2008) rejected membership in ϵ Cha on the basis of a $-3.3 \pm 1.0\,\mathrm{km\,s^{-1}}$ velocity from Guenther et al. (2007), but this was almost certainly not systemic, nor is the mean WiFeS value. At its 106 pc kinematic distance RX J1150.4−7704 lies 1.4 mag below the isochrone, more if its unresolved companion contributes significantly to the *I*-band flux. Despite strong lithium absorption and a congruent proper motion, we rule out membership in ϵ Cha. A systemic velocity would be useful. Wahhaj et al. (2010) classified the star as T Tauri based on a broad Hα line, but this is likely the result of binarity.

2MASS J12074597−7816064 (ϵ Cha 12) – a proper motion outlier, ϵ Cha 12 also shows evidence of spectroscopic binarity. We find a good match to the ϵ Cha space motion at 85 pc, but the star is underluminous at this distance. It is located in the core of the association and its strong lithium absorption implies an age comparable to other members. The companion, if it exists, may have influenced the star's proper motions but even at 110 pc ϵ Cha 12 remains significantly underluminous. We refrain from assigning it to ϵ Cha pending better kinematics and confirmation of binarity.

RX J1123.2−7924 (ϵ Cha 14) – Lopez Martí et al. (2013) reaffirmed membership in ϵ Cha based on a marginally consistent proper motion. However, the star's low Li I EW (130 mÅ) and position below the isochrone mean this is unlikely. The proper motion may have been influenced by the spectroscopic companion, but we did find an good kinematic match to the $\sim$20 Myr old Octans association (Torres et al. 2008) at 110 pc. The lithium depletion, CMD placement and heliocentric position of RX J1123.2−7924 are consistent with this assignment.

A4 Candidates without radial velocities

Five candidates lack any radial velocity information. To calculate kinematic distances for these stars, we compared their proper motions to the ϵ Cha solution or used parallaxes if available. TYC 9414-191-1, HD 105234 and HIP 59243 may be members based on their kinematic match and CMD placement. Radial velocities and a Li I λ6708 measurement for TYC 9414-191-1 are necessary to confirm membership. The two remaining Tycho sources (TYC 9420-676-1, TYC 9238-612-1) have positions below the empirical isochrone and are unlikely to be members.

APPENDIX B: CANDIDATE MEASUREMENTS

The astrometric and spectroscopic measurements adopted for each candidate are listed in Table B1 with appropriate references. NIR photometry from DENIS, 2MASS and *WISE* is given in Table B2.

Table B1. Adopted astrometry and spectroscopic measurements of ϵ Cha candidates. Spectral types, velocities and EW measurements are derived from our WiFeS spectroscopy unless specified.

ID	Name	RA (J2000)	Dec. (J2000)	Spectral type	Reference[a]	$E(B-V)$ (mag)	RV (km s^{-1})	Reference[a]	Li I EW (mÅ)	Reference[a]	Hα EW (Å)	Reference[a]	$\mu_\alpha \cos\delta$ (mas yr^{-1})	μ_δ (mas yr^{-1})	Reference[b]
	HD 82879	09 28 21.1	−78 15 35.0	F6	T08	0.0	16.8 ± 2.0	C97	100 ± 15	C97	4.5	C97	−24.0 ± 1.4	21.3 ± 1.4	TYC
	CP−68 1388	10 57 49.3	−69 14 00.0	K1	T08	0.1	15.9 ± 1.0	T06	420 ± 15	dS09	0.0	T08	−36.1 ± 2.4	5.7 ± 2.3	TYC
	VW Cha	11 08 01.5	−77 42 29.0	K8	LL04	1.0	17.2 ± 0.5	G07	440 ± 50	G07	−64.0	M11	−18.9 ± 1.3	−2.0 ± 1.8	UCAC4
	TYC 9414-191-1	11 16 29.0	−78 25 20.8	K5		0.3	–	–	–	–	–	–	−39.8 ± 3.0	−4.5 ± 2.9	TYC
13	2MASS J11183572−7935548	11 18 35.7	−79 35 54.8	M4.5		0.0	19.3 ± 1.6		600 ± 50		[−30.0, −18.0]		−41.9 ± 1.5	3.1 ± 1.6	SPM4
14	RX J1123.2−7924	11 22 55.6	−79 24 43.8	M1.5		0.0	2.7 ± 2.9		130 ± 15	C97	−2.0		−30.6 ± 1.3	−16.8 ± 1.3	SPM4
	HIP 55746	11 25 18.1	−84 57 16.0	F5	T08	0.0	21.1 ± 1.2	N04	80 ± 15	C97	4.0	C97	−48.4 ± 0.7	12.0 ± 0.6	HIP
15	2MASS J11334926−7618399	11 33 49.3	−76 18 39.9	M4.5		0.15	16.7 ± 1.5		650 ± 50		−6.0		−21.7 ± 2.7	1.6 ± 2.8	SPM4
	RX J1137.4−7648	11 37 31.3	−76 47 59.0	M2.2		0.0	14.0 ± 5.0		0		−1.5		−64.3 ± 1.2	3.4 ± 1.3	SPM4
16	2MASS J11404967−7459394	11 40 49.7	−74 59 39.4	M5.5		0.0	10.3 ± 1.0		700 ± 50		[−35.0, −11.0]		−41.7 ± 8.8	5.2 ± 9.1	SPM4
	TYC 9238-612-1	11 41 27.7	−73 47 03.0	G5	ZS04	0.05	–	–	–	–	–	–	−34.9 ± 2.0	9.5 ± 1.9	TYC
17	2MASS J11432669−7804454	11 43 26.7	−78 04 45.4	M4.7		0.05	15.6 ± 1.0		700 ± 50		[−120.0, −60.0]		−36.7 ± 2.3	1.4 ± 2.3	SPM4
	RX J1147.7−7842	11 47 48.1	−78 41 52.0	M3.5		0.0	16.1 ± 0.9		650 ± 50		[−7.0, −4.0]		−39.9 ± 1.8	−6.5 ± 1.8	SPM4
18	RX J1149.8−7850	11 49 31.8	−78 51 01.1	M0	T08	0.3	13.4 ± 1.3	T06	560 ± 15	dS09	−32.0	C97	−39.1 ± 1.8	−4.5 ± 1.8	SPM4
19	RX J1150.4−7704	11 50 28.3	−77 04 38.0	K4		0.0	6.1 ± 1.6		420 ± 15	C97	−1.0		−39.7 ± 1.1	−8.9 ± 1.2	SPM4
	RX J1150.9−7411	11 50 45.2	−74 11 13.0	M3.7		0.0	15.0 ± 1.2		500 ± 50		−8.0		−39.0 ± 4.2	4.4 ± 2.9	T99
	2MASS J11550485−7919108	11 55 04.9	−79 19 10.9	M3	K12	0.5	14.0 ± 1.3	TCha	550 ± 50	K12	−6.5	K12	−37.7 ± 3.7	0.7 ± 3.7	SPM4
	T Cha	11 57 13.5	−79 21 31.5	K0	K12	0.5	14.0 ± 1.3	G07	360 ± 15	dS09	[−30.0, 0.0]	S09	−40.2 ± 1.5	−4.6 ± 1.4	SPM4
20	RX J1158.5−7754B	11 58 26.8	−77 54 45.0	M3	T08	0.0	13.0 ± 2.0	C97	600 ± 15	dS09	−3.0	C97	−36.0 ± 1.0	−6.6 ± 1.0	SPM4
21	RX J1158.5−7754A	11 58 28.2	−77 54 29.6	K4		0.0	10.2 ± 0.2	J06	483 ± 15	T06	−0.5		−41.7 ± 1.6	0.1 ± 1.4	HIP
	HD 104036	11 58 35.2	−77 49 32.0	A7	M00	0.0	12.4 ± 1.0	G99	0	dS09	–	–	−41.6 ± 0.4	−8.8 ± 0.3	HIP
1	CXOU J115908.2−781232	11 59 08.0	−78 12 32.2	M4.75	L04	0.0	15.1 ± 0.2		650 ± 50		−5.0		−25.4 ± 2.4	4.0 ± 2.4	SPM4
2	ϵ Cha AB	11 59 37.5	−78 13 18.9	B9	T08	0.0	13.0 ± 5.0	BB00	0	dS09	13.0	F03	−40.3 ± 0.4	−8.3 ± 0.4	HIP
	RXJ1159.7-7601	11 59 42.3	−76 01 26.2	K4	T08	0.0	13.8 ± 0.1	G07	445 ± 15	dS09	−0.4	C97	−40.5 ± 1.7	−5.8 ± 1.5	HIP
5	HD 104237A	12 00 05.1	−78 11 34.6	A7.75	L04	0.2	14.0 ± 1.0	G04	0	dS09	−20.0	F03	−39.0 ± 0.4	−5.8 ± 0.3	HIP
6	HD 104237D	12 00 08.3	−78 11 39.6	M3.5	L04	0.0	13.4 ± 1.0	G04	580 ± 15	dS09	−3.9	F03	−35.7 ± 5.5	18.8 ± 5.6	SPM4
7	HD 104237E	12 00 09.3	−78 11 42.5	K5.5	L04	0.3	13.4 ± 1.0	G04	480 ± 15	dS09	−4.5	F03	−1.8 ± 4.2	4.4 ± 4.2	SPM4
10	2MASS J12005517−7820296	12 00 55.2	−78 20 29.7	M5.75	L04	0.0	10.7 ± 1.3		600 ± 50		[−20.0, −10.0]		−34.5 ± 3.7	0.9 ± 3.7	SPM4
	HD 104467	12 01 39.1	−78 59 16.9	G3	T08	0.0	12.3 ± 1.4	T06	260 ± 15	dS09	0.0	T06	−42.8 ± 1.4	−4.0 ± 1.3	TYC
11	2MASS J12014343−7835472	12 01 43.4	−78 35 47.2	M2.25	L04	0.0	20.0 ± 0.6		700 ± 50		[−140.0, −70.0]		−43.1 ± 8.8	−6.5 ± 8.8	PPMXL
8	USNO-B 120144.7−781926	12 01 44.4	−78 19 26.8	M5	L04	0.0	14.9 ± 1.1		500 ± 50		[−45.0, −20.0]		−43.7 ± 4.9	−1.6 ± 4.9	SPM4

Table B1 – *continued*

ID	Name	RA (J2000)	Dec. (J2000)	Spectral type	Reference[a]	$E(B-V)$ (mag)	RV (km s^{-1})	Reference[a]	Li I EW (mÅ)	Reference[a]	Hα EW (Å)	Reference[a]	$\mu_\alpha \cos\delta$ (mas yr^{-1})	μ_δ (mas yr^{-1})	Reference[b]
9	CXOU J120152.8−781840	12 01 52.5	−78 18 41.4	M4.75	L04	0.0	16.5 ± 1.1		650 ± 50		−8.0		−35.2 ± 4.2	− 7.3 ± 4.1	SPM4
	RX J1202.1−7853	12 02 03.8	−78 53 01.0	M0	T08	0.0	17.1 ± 0.2	G07	540 ± 15	dS09	−2.5	C97	−39.5 ± 1.5	− 2.0 ± 1.5	SPM4
	RX J1202.8−7718	12 02 54.6	−77 18 38.2	M3.5		0.0	17.1 ± 1.2		300 ± 50		[−12.0, −5.0]		−34.2 ± 1.2	− 2.6 ± 1.4	SPM4
	RX J1204.6−7731	12 04 36.1	−77 31 34.6	M3	R06	0.0	10.4 ± 2.0	C97	470 ± 15	dS09	−4.2	C97	−38.8 ± 1.2	− 2.9 ± 1.3	SPM4
	TYC 9420-676-1	12 04 57.4	−79 32 04.7	F0	M00	0.2	–	–	–	–	–	–	−40.2 ± 1.4	− 0.5 ± 1.3	TYC
	HD 105234	12 07 05.5	−78 44 28.1	A9	M00	0.0	–	–	–	–	–	–	−41.6 ± 0.6	− 9.4 ± 0.4	HIP
12	2MASS J12074597−7816064	12 07 46.0	−78 16 06.5	M3.75	L04	0.0	15.2 ± 1.9		500 ± 50		−3.5		−48.8 ± 2.1	− 14.2 ± 2.1	SPM4
	RX J1207.7−7953	12 07 48.3	−79 52 42.0	M3.5		0.0	15.0 ± 0.7		550 ± 50		−4.0		−39.0 ± 1.8	− 6.2 ± 1.8	SPM4
	HIP 59243	12 09 07.8	−78 46 53.0	A6	ZS04	0.05	–	–	–	–	–	–	−43.0 ± 0.4	− 7.7 ± 0.3	HIP
	HD 105923	12 11 38.1	−71 10 36.0	G8	T08	0.15	14.2 ± 1.0	T06	280 ± 15	dS09	–	–	−38.9 ± 1.4	− 8.3 ± 1.4	TYC
	RX J1216.8−7753	12 16 45.9	−77 53 33.0	M4	C97	0.0	14.0 ± 2.0	C97	550 ± 15	C97	−4.0	C97	−36.5 ± 1.2	− 7.6 ± 1.3	SPM4
	RX J1219.7−7403	12 19 43.7	−74 03 57.3	M0	C97	0.0	13.8 ± 0.1	G07	560 ± 15	dS09	−3.3	C97	−39.0 ± 1.3	− 8.0 ± 1.5	SPM4
	RX J1220.4−7407	12 20 21.8	−74 07 39.4	M0	C97	0.0	12.3 ± 0.4	G07	610 ± 15	dS09	−2.2	C97	−40.1 ± 1.5	− 6.2 ± 1.7	SPM4
	2MASS J12210499−7116493	12 21 04.9	−71 16 49.3	K7	R06	0.0	11.5 ± 1.4	K11	550 ± 20	K11	−0.8	K11	−39.4 ± 1.1	− 11.8 ± 1.2	SPM4
	RX J1239.4−7502	12 39 21.3	−75 02 39.2	K3	C97	0.05	13.9 ± 0.2	G07	459 ± 15	dS09	0.1	C97	−43.6 ± 2.0	− 11.1 ± 1.9	TYC
	RX J1243.1−7458	12 42 53.1	−74 58 49.0	M3.2		0.0	13.5 ± 0.7		600 ± 15	C97	[−7.0, −4.0]		−14.2 ± 1.9	− 5.6 ± 2.2	SPM4
	CD−69 1055	12 58 25.6	−70 28 49.0	K0	T08	0.15	12.8 ± 1.0	T06	400 ± 15	dS09	−0.2	T06	−43.1 ± 1.5	− 18.7 ± 1.5	TYC
	CM Cha	13 02 13.6	−76 37 58.0	K7	T06	0.5	15.9 ± 1.1	T06	520 ± 15	T06	−29.0	S08	−33.0 ± 2.7	− 5.7 ± 2.9	SPM4
	MP Mus	13 22 07.6	−69 38 12.0	K1	T08	0.05	11.6 ± 0.2	T06	424 ± 15	dS09	−37.0	T06	−40.8 ± 2.5	− 23.0 ± 2.3	TYC

[a]References: (T06) Torres et al. (2006), (T08) Torres et al. (2008), (L04) Luhman (2004b), (LL04) Luhman (2004a), (ZS04) Zuckerman & Song (2004), (K12) Kastner et al. (2012), (M00) Mamajek et al. (2000), (R06) Riaz, Gizis & Harvin (2006), (C97) Covino et al. (1997), (G07) Guenther et al. (2007), (N04) Nordström et al. (2004), (TCha) Same velocity as T Cha, (J06) James et al. (2006), (G99) Grenier et al. (1999), (BB00) Barbier-Brossat & Figon (2000), (G04) Grady et al. (2004), (K11) Kiss et al. (2011), (dS09) da Silva et al. (2009), (M11) Manoj et al. (2011), (S09) Schisano et al. (2009), (F03) Feigelson et al. (2003), (S08) Spezzi et al. (2008).

[b]Proper motion references: (TYC) Tycho-2/Høg et al. (2000), (HIP) *Hipparcos*/van Leeuwen (2007), (UCAC4) Zacharias et al. (2013), (SPM4) Girard et al. (2011), (PPMXL) Röser et al. (2010).

Table B2. Adopted photometry for ϵ Cha candidates. Unless specified, *I*-band data is from the DENIS survey (Epchtein et al. 1999) with JHK_s from 2MASS (Skrutskie et al. 2006) and *W*1, *W*2, *W*3, *W*4 from *WISE* (Wright et al. 2010).

ID	Name	*I* (mag)	Reference[a]	*J* (mag)	*H* (mag)	K_s (mag)	Reference[a]	*W*1 (mag)	*W*2 (mag)	*W*3 (mag)	*W*4 (mag)
	HD 82879	8.95		8.12	7.93	7.83		7.78	7.80	7.82	7.92
	CP−68 1388	9.28	T06	8.48	8.01	7.79		7.72	7.74	7.68	7.59
	VW Cha	11.03	B01	8.70	7.64	6.96		6.15	5.40	4.12	1.85
	TYC 9414-191-1	9.59		8.41	7.76	7.53		7.43	7.55	7.45	7.43
13	2MASS J11183572−7935548	12.22		10.49	9.89	9.62		9.42	9.14	7.67	4.47
14	RX J1123.2−7924	11.62		10.52	9.84	9.67		9.52	9.46	9.31	8.61
	HIP 55746	7.15	[b]	6.73	6.57	6.49		6.40	6.44	6.46	6.41
15	2MASS J11334926−7618399	14.08		12.15	11.50	11.18		11.08	10.86	10.72	8.90
	RX J1137.4−7648	12.20	[d]	11.85	10.48	10.14		9.80	9.70	9.59	8.94
16	2MASS J11404967−7459394	15.02		12.68	12.15	11.77		11.58	11.31	11.04	9.31
	TYC 9238-612-1	9.98		9.39	9.02	8.86		8.78	8.80	8.74	8.49
17	2MASS J11432669−7804454	13.51		11.62	10.97	10.60		10.23	9.84	8.71	7.12
	RX J1147.7−7842	10.92		9.52	8.86	8.59		8.47	8.33	8.22	8.42
18	RX J1149.8−7850	11.01		9.45	8.72	8.49		8.20	7.67	4.54	1.82
19	RX J1150.4−7704	10.54		9.71	9.13	8.97		8.86	8.87	8.79	8.71
	RX J1150.9−7411	12.06	[b]	10.60	9.78	9.48		9.31	9.14	8.98	8.64
	2MASS J11550485−7919108	13.26		11.22	10.46	10.08		9.87	9.65	9.27	6.84
	T Cha	10.28		8.96	7.86	6.95		5.84	5.01	4.66	2.56
20	RX J1158.5−7754B	11.81		10.34	9.71	9.44		9.35	9.20	9.08	8.75
21	RX J1158.5−7754A	9.76	[b]	8.63	7.56	7.40		7.27	7.28	7.19	7.08
	HD 104036	6.49	HIP	6.29	6.22	6.11		6.10	6.08	6.13	6.08
1	CXOU J115908.2−781232	13.83	F03	12.01	11.45	11.17		10.97	10.74	10.19	8.32
2	ϵ Cha A	5.39	F03[c]	5.52	5.04	4.98		5.25	4.97	5.11	4.84
	RX J1159.7−7601	10.18		9.14	8.47	8.30		8.16	8.19	8.08	7.85
3	HD 104237C	–	–	15.28	14.85	14.48	G04	–	–	–	–
4	HD 104237B	–	–	11.43	10.27	9.52	G04	–	–	–	–
5	HD 104237A	6.31	HIP	5.81	5.25	4.58		3.89	2.47	0.93	-0.91
6	HD 104237D	11.62	F03	10.53	9.73	9.67	G04	–	–	–	–
7	HD 104237E	10.28	F03	9.10	8.05	7.70	G04	–	–	–	–
10	2MASS J12005517−7820296	14.00		11.96	11.40	11.01		10.62	10.16	8.52	6.61
	HD 104467	7.81	T06	7.26	6.97	6.85		6.81	6.80	6.78	6.82
11	2MASS J12014343−7835472	15.96		14.36	13.38	12.81		12.36	11.60	7.59	5.24
8	USNO-B 120144.7−781926	13.72	F03	11.68	11.12	10.78		10.16	9.74	8.35	6.70
9	CXOU J120152.8−781840	13.52	F03	11.63	11.04	10.77		10.57	10.35	10.05	9.32
	RX J1202.1−7853	10.49		9.21	8.46	8.31		8.10	8.04	7.92	8.13
	RX J1202.8−7718	11.90		10.51	9.82	9.59		9.53	9.40	9.20	8.78
	RX J1204.6−7731	11.25		9.77	9.12	8.88		8.74	8.59	8.50	8.81
	TYC 9420-676-1	9.73		9.24	9.09	8.94		8.86	8.88	8.86	9.15
	HD 105234	7.17	HIP	6.87	6.76	6.68		6.55	6.48	5.43	4.57
12	2MASS J12074597−7816064	13.11		11.55	10.98	10.67		10.50	10.33	10.19	8.88
	RX J1207.7−7953	12.06		10.43	9.76	9.57		9.45	9.31	9.24	8.62
	HIP 59243	6.56	HIP	6.34	6.23	6.17		6.11	6.12	6.16	6.05
	HD 105923	8.31	T06	7.67	7.31	7.17		7.07	7.08	7.04	6.96
	RX J1216.8−7753	11.65		10.09	9.46	9.24		9.14	9.03	8.91	8.76
	RX J1219.7−7403	10.95		9.75	9.05	8.86		8.75	8.67	8.54	8.28
	RX J1220.4−7407	10.80	[b]	9.43	8.61	8.37		8.26	8.15	8.04	8.11
	2MASS J12210499−7116493	10.21		9.09	8.42	8.24		8.16	8.16	8.08	7.99
	RX J1239.4−7502	9.21	T06	8.43	7.95	7.78		7.72	7.75	7.71	7.45
	RX J1243.1−7458	12.72	[b]	11.27	10.15	9.81		9.54	9.37	9.34	9.48
	CD−69 1055	8.89	T06	8.18	7.70	7.54		7.43	7.47	7.42	7.44
	CM Cha	11.80	T06	10.02	9.16	8.52		7.62	7.16	5.06	3.06
	MP Mus	9.18	T06	8.28	7.64	7.29		6.58	6.18	4.06	1.59

[a]Photometry references: (T06) SACY/Torres et al. (2006), (HIP) *Hipparcos* catalogue (Perryman et al. 1997), (F03) Feigelson et al. (2003), (G04) Grady et al. (2004), (B01) Brandeker et al. (2001).

[b]DENIS *I* and 2MASS *J* photometry corrected for multiplicity using the *K*-band flux ratios of Köhler (2001) and main-sequence colours of Kraus & Hillenbrand (2007).

[c]F03 *I* and 2MASS *J* photometry corrected for multiplicity using the *V*-band magnitudes in Feigelson et al. (2003) and main-sequence colours of Kraus & Hillenbrand (2007).

[d]DENIS *I* and 2MASS *J* photometry corrected assuming an equal-mass system.

This paper has been typeset from a TEX/LATEX file prepared by the author.